7. De Marzo AM, Platz EA, Sutcliffe S *et al.*: Inflammation in prostate carcinogenesis. *Nat. Rev. Cancer* 7, 256–269 (2007).
8. Sun J, Turner A, Xu J, Gronberg H, Isaacs W: Genetic variability in inflammation pathways and prostate cancer risk. *Urol. Oncol.* 25, 250–259 (2007).
9. Listowsky I, Abramovitz M, Homma H, Niitsu Y: Intracellular binding and transport of hormones and xenobiotics by glutathione-*S*-transferases. *Drug. Metab. Rev.* 19, 305–318 (1998).
10. Hayes JD, Pulford DJ: The glutathione *S*-transferase supergene family: regulation of GST and the contribution of the isoenzymes to cancer chemoprotection and drug resistance. *Crit. Rev. Biochem. Mol. Biol.* 30, 445–600 (1995).
11. Hayes JD, Strange RC: Glutathione-*S*-transferase polymorphisms and their biological consequence. *Pharmacology* 61, 154–166 (2000).
12. Hayes JD, Flanagan JU, Jowsey IR: Glutathione transferases. *Annu. Rev. Pharmacol. Toxicol.* 45, 51–88 (2005).
•• Recent review with extensive discussion on glutathione S-transferase (GST).
13. Mannervik KB, Alin P, Guthenberg C *et al.*: Nomenclature for human glutathione-*S*-transferases. *Biochem. J.* 282, 305–306 (1992).
14. Seidegard J, Pero RW, Miller DG, Beattie EJ: A glutathione-S-transferase in human leukocytes as a marker for the susceptibility to lung cancer. *Carcinogenesis.* 7: 751–753 (1986).
15. Autrup JL, Thomassen LH, Olsen JH, Wolf H, Autrup H: Glutathione *S*-transferases as risk factors in prostate cancer. *Eur. J. Cancer Prev.* 8, 525–32 (1999)
16. Rebbeck TR, Walker AH, Jaffe JM, White DL, Wein AJ, Malkowicz B: Glutathione *S*-transferase-μ (*GSTM1*) and -τ (*GSTT1*) genotypes in the etiology of prostate cancer. *Cancer Epidemiol. Biomarkers Prev.* 8, 283–287 (1999).
17. Shepard TF, Platz EA, Kantoff PW *et al.*: No association between the I105V polymorphism of the glutathione *S*-transferase P1 gene (*GSTP1*) and prostate cancer risk: a prospective study. *Cancer Epidemiol. Biomarkers Prev.* 9, 1267–1268 (2000).
18. Steinhoff C, Frank KH, Golka K *et al.*: Glutathione transferase isozyme genotypes in patients with prostate and bladder carcinoma. *Arch. Toxicol.* 74, 521–526 (2000).
19. Gsur A, Haidinger G, Hinteregger S *et al.*: Polymorphisms of glutathione-*S*-transferase genes (*GSTP1*, *GSTM1* and *GSTT1*) and prostate-cancer risk. *Int. J. Cancer* 95: 152–155 (2001).
20. Kote-Jarai Z, Easton D, Edwards SM *et al.*: Relationship between glutathione *S*-transferase M1, P1 and T1 polymorphisms and early onset prostate cancer. *Pharmacogenetics* 11, 325–330 (2001).
21. Jerónimo C, Varzim G, Henrique R *et al.*: I105V polymorphism and promoter methylation of the *GSTP1* gene in prostate adenocarcinoma. *Cancer Epidemiol. Biomarkers Prev.* 11, 445–450 (2002).
22. Kidd LC, Woodson K, Taylor PR, Albanes D, Virtamo J, Tangrea JA: Polymorphisms in glutathione-*S*-transferase genes (*GST-M1*, *GST-T1* and *GST-P1*) and susceptibility to prostate cancer among male smokers of the ATBC cancer prevention study. *Eur. J. Cancer Prev.* 12, 317–320 (2003).
23. Acevedo C, Opazo JL, Huidobro C, Cabezas J, Iturrieta J, Quinones Sepulveda L: Positive correlation between single or combined genotypes of *CYP1A1* and *GSTM1* in relation to prostate cancer in Chilean people. *Prostate* 57, 111–117 (2003).
24. Debes JD, Yokomizo A, McDonnell SK *et al.*: Gluthatione-*S*-transferase P1 polymorphism I105V in familial and sporadic prostate cancer. *Cancer Genet. Cytogenet.* 155, 82–86 (2004).
25. Medeiros R, Vasconcelos A, Costa S *et al.*: Metabolic susceptibility genes and prostate cancer risk in a southern European population: the role of glutathione *S*-transferases *GSTM1*, *GSTM3*, and *GSTT1* genetic polymorphisms. *Prostate* 58, 414–420 (2004).
26. Shankar D, Srivastava L, Mandhni A, Mittal B, Mittal RD: Genetic polymorphism of glutathione *S*-transferase genes (*GSTM1*, *GSTT1* and *GSTP1*) and susceptibility to prostate cancer in Northern India. *BJU Int.* 95, 170–173 (2005).
27. Agalliu I, Lin DW, Salinas CA, Feng Z, Stanford JL: Polymorphisms in the glutathione *S*-transferase M1, T1, and P1 genes and prostate cancer prognosis. *Prostate* 66, 1535–1541 (2006).
28. Watson MA, Stewart RK, Smith GB, Massey TE, Bell DA: Human glutathione *S*-transferase P1 polymorphisms: relationship to lung tissue enzyme activity and population frequency distribution. *Carcinogenesis* 19, 275–280 (1998).
29. Sweeney C, Ambrosone CB, Joseph L *et al.*: Association between a glutathione *S*-transferase A1 promoter polymorphism and survival after breast cancer treatment. *Int. J. Cancer* 103, 810–814 (2003).
30. Ning B, Wang C, Morel F *et al.*: Human glutathione *S*-transferase A2 polymorphisms: variant expression, distribution in prostate cancer cases/controls and a novel form. *Pharmacogenetics* 14, 35–44 (2004).
31. London SJ, Daly AK, Cooper J, Navidi WC, Carpenter CL, Idle JR: Polymorphism of glutathione S-transferase M1 and lung cancer risk among African–Americans and Caucasians in Los Angeles County, California. *J. Natl. Cancer Inst.* 87, 1246–1253 (1995).
32. Murata M, Shiraishi T, Fukutome K *et al.*: Cytochrome P4501A1 and glutathione *S*-transferase M1 genotypes as risk factors for prostate cancer in Japan. *Jpn. J. Clin. Oncol.* 28, 657–660 (1998).
33. Nakazato H, Suzuki K, Matsui H *et al.*: Association of genetic polymorphisms of glutathione-*S*-transferase genes (*GSTM1*, *GSTT1* and *GSTP1*) with familial prostate cancer risk in a Japanese population. *Anticancer Res.* 23, 2897–2902 (2003).
34. Komiya Y, Tsukino H, Nakao H, Kuroda Y, Imai H, Katoh T: Human glutathione *S*-transferase A1, T1, M1, and P1 polymorphisms and susceptibility to prostate cancer in the Japanese population. *J. Cancer Res. Clin. Oncol.* 131, 238–42 (2005).
35. Seidegard J, Vorachek WR, Pero RW, Pearson WR: Hereditary differences in the expression of the human glutathione transferase active on trans-stilben oxide are due to a gene deletion. *Proc. Natl. Acad. Sci. USA* 85, 7203–7207 (1998).
36. Widersten M, Pearson WR, Engstrom A, Mannervik B: Heterologous expression of the allelic variant μ-class glutathione transferase μ and ψ. *Biochem. J.* 276, 519–524 (1991).
37. Inskip A, Elexperu-Camiruaga J, Buxton N *et al.*: Identification of polymorphism at the glutathione *S*-transferase, *GSTM3* locus: evidence for linkage with *GSTM1*A Biochem. J.* 312, 713–716 (1995).
38. Pemble S, Schreoder KR, Spencer SR *et al.*: Human glutathione-*S*-transferases τ: cDNA cloning and the characterization of polymorphism. *Biochem. J.* 300, 271–276 (1994).
39. Lof A, Johanson G, Rannug A, Warholm M: Glutathione transferase T1 phenotype affects the toxicokinetics of inhaled methyl chloride in human volunteers. *Pharmacogenetics* 10, 645–653 (2000).

40. Their R, Lewalten J, Kempkes M, Selinski S, Bruning T, Bolt HM: Haemoglobin adducts of acrylonitrile and ethylene oxide in acrylonitrile workers dependent on polymorphisms of the glutathione transferases GSTT1 and GSTM1. *Arch. Toxicol.* 73, 197–202 (1999).
41. Terrier P, Townsend AJ, Coindre JM, Triche TJ, Cowan KH: An immunohistochemical study of pi class glutathione S-transferase expression in normal human tissue. *Am. J. Pathol.* 137, 845–853 (1990).
42. De Weese TL, Hruszkewycz AM, Marnett LJ: Oxidative stress in chemoprevention trials. *Urology* 57, 137–140 (2001).
43. Nelson WG, De Marzo AM, De Weese TL: The molecular pathogenesis of prostate cancer: implications for prostate cancer prevention. *Urology* 57, 39–45 (2001).
44. Ali-Osman F, Akande O, Antoun G, Mao JX, Buolamwini J: Molecular cloning, characterization, and expression in Escherichia coli of full-length cDNAs of three human glutathione *S*-transferase Pi gene variants. Evidence for differential catalytic activity of the encoded proteins. *J. Biol. Chem.* 272, 10004–10012 (1997).
45. Coles BF, Morel F, Rauch C *et al.*: Effect of polymorphism in the human glutathione *S*-transferase A1 promoter on hepatic *GSTA1* and *GSTA2* expression. *Pharmacogenetics* 11, 663–669 (2001).
46. Parsons JK, Nelson CP, Gage WR, Nelson WG, Kensler TW, De Marzo AM: *GSTA1* expression in normal, preneoplastic, and neoplastic human prostate tissue. *Prostate* 49, 30–37 (2001).
47. Coles B, Nowell SA, MacLeod SL, Sweeney C, Lang NP, Kadlubar FF: The role of human glutathione *S*-transferases (hGSTs) in the detoxification of the food-derived carcinogen metabolite *N*-acetoxy-PhIP, and the effect of a polymorphism in *hGSTA1* on colorectal cancer risk. *Mutat. Res.* 482, 3–10 (2001).
48. Morel F, Rauch C, Coles B, Le Ferrec E, Guillouzo A: The human glutathione transferase α locus: genomic organization of the gene cluster and functional characterization of the genetic polymorphism in the *hGSTA1* promoter. *Pharmacogenetics* 12, 277–286 (2002).
49. Board P: Ligandin revisited: resolution of the α class glutathione transferase gene family. *Pharmacogenetics* 12, 275–276 (2002).
50. Kelada SN, Kardia SL, Walker AH, Wein AJ, Malkowicz SB, Rebbeck TR: The glutathione *S*-transferase-μ and -τ genotypes in the etiology of prostate cancer: genotype-environment interactions with smoking. *Cancer Epidemiol. Biomarkers Prev.* 9, 1329–1334 (2000).
51. Ntais C, Polycarpou A, Ioannidis JP: Association of *GSTM1*, *GSTT1*, and *GSTP1* gene polymorphisms with the risk of prostate cancer: a meta-analysis. *Cancer Epidemiol. Biomarkers Prev.* 14, 176–181 (2005).
•• Meta-analyses in studies of the relationship between *GSTM1*, *GSTT1* and *GSTP1*, and prostate cancer.
52. Nelson CP, Kidd LC, Sauvageot J *et al.*: Protection against 2-hydroxyamino-1-methyl-6-phenylimidazo[4,5-b]pyridine cytotoxicity and DNA adduct formation in human prostate by glutathione S-transferase P1. *Cancer Res.* 61, 103–109 (2001).
53. Bartsch H, Nair U, Risch A, Rojas M, Wikman H, Alexandrov K: Genetic polymorphism of CYP genes, alone or in combination, as a risk modifier of tobacco-related cancers. *Cancer Epidemiol Biomarkers Prev.* 9, 3–28 (2000).

Induction of multinucleated cells and apoptosis in the PC-3 prostate cancer cell line by low concentrations of polyethylene glycol 1000

Katsuhiro Fukuta,[1,2] Kenjiro Kohri,[2] Hirokazu Fukuda,[1] Masatoshi Watanabe,[3] Takashi Sugimura[1] and Hitoshi Nakagama[1,4]

[1]Biochemistry Division, National Cancer Center Research Institute, 5-1-1, Tsukiji, Chuo-ku, Tokyo 104-0045; [2]Department of Nephro-Urology, Nagoya City University Graduate School of Medical Sciences, 1, Kawasumi, Mizuho-cho, Mizuho-ku, Nagoya 467-8601; [3]Laboratory for Medical Engineering, Division of Materials Science and Chemical Engineering, Graduate School of Engineering, Yokohama National University, 79-1 Tokiwadai, Hodogaya-ku, Yokohama 240-8501, Japan

(Received December 27, 2007/Revised January 16, 2008/Accepted January 17, 2008/Online publication March 28, 2008)

Polyethylene glycol (PEG) has been reported to inhibit the development of colonic lesions in carcinogen-treated rats when administered orally. However, the precise mechanism for the chemopreventive activity of PEG remains largely elusive. Based on a characteristic feature of PEG as a 'fusogen', we investigated its potential as a chemotherapeutic agent through the induction of multinucleated cell formation and apoptosis induction in PC-3 prostate cancer cells. When PC-3 cells were treated with 0.5 and 1.0% PEG 1000, multinucleated cells were induced at a frequency of 8.4 and 13%, respectively, 36 h after PEG treatment under high cell density (1×10^6 cells in 100 μL PEG solution) *in vitro*. Although abnormality of cell cycle progression was not evident in PEG-treated PC-3 cells, multinucleated cells substantially disappeared at around 38 h due to apoptosis. In contrast, no apparent growth suppression was observed when PC-3 cells were exposed to up to 1.0% PEG at a much lower cell density, namely under ordinary culture conditions. Furthermore, injection of 0.5% PEG solution *in vivo* into PC-3 xenografts implanted in BALB/c-nu/nu male mice significantly suppressed tumor growth compared to phosphate-buffered saline injection. Multinucleated TdT-mediated dUTP-biotin nick end-labeling (TUNEL)-positive cells were observed inside the PEG-injected tumors. PEG was here demonstrated to have anticell proliferation and antitumor effects via induction of apoptosis, possibly by cell fusion. PEG injection therapy could therefore be adopted as an alternative chemotherapeutic strategy for localized prostate cancers, including those that become refractory to androgen-deprivation therapy. (*Cancer Sci* 2008; 99: 1055–1062)

Polyethylene glycol (PEG) has the chemical structure $H\text{-}(O\text{-}CH_2\text{-}CH_2)_n\text{-}OH$, and is known to be a nonabsorbed, non-toxic, and non-fermentable polymer.[1,2] Because PEG is non-toxic, it is used widely as a base material in, for example, skin creams and laxatives.[3,4] When PEG is bound to a hydrophobic molecule, a non-ionic detergent surfactant is obtained and can be used as an emulsion agent in cosmetics.[5] PEG is also used to encapsulate and solubilize hydrophobic compounds. It has recently been utilized in drug delivery systems, and PEGylation of interferon α (peginterferon α) and granulocyte colony-stimulating factor (pegfilgrastim) are now used for clinical applications.[6,7] The stability and hydrosolubility of various drugs is thereby markedly improved even under *in vivo* conditions. In the research field of biotechnology, PEG is also used for cell fusion as a 'fusogen'.[8,9]

In addition to these features, chemopreventive effects of PEG have been reported in rodent models of colon cancer.[10,11] When rats were treated with PEG 8000 after the administration of azoxymethane, a widely utilized colon carcinogen, a substantial decrease was observed in the number of aberrant crypt foci, putative precancerous lesions of the colon, and colon tumors.[12] Although the mechanistic interpretation for the chemopreventive effect of PEG is still controversial, several possibilities have been proposed. First, an increase in the gut content because of the high osmotic pressure in the digestive tract caused by the non-absorbed high molecular weight PEG could be a possibility, similar to dietary fiber.[10,13,14] Another possibility is that PEG may act directly on colon epithelial cells and exert some biological effects, such as induction of apoptosis, through osmotic pressure.[15]

In the present study, we examined whether PEG induces apoptosis in cancer cells using an androgen-independent human prostate cancer cell line, PC-3,[16] and could be used as an alternative therapeutic agent for human prostate cancers. Prostate cancer is a common cancer in men all over the world, and its incidence in Japan is currently increasing.[17,18] As for prostate cancer therapies, androgen-deprivation therapy (hormone therapy) now prevails all over the world, as it is non-invasive and relatively effective in many cases.[19–21] Radiation therapy, such as 'brachytherapy', is also used for localized prostate cancer.[22] However, these therapies have some drawbacks. For example, brachytherapy requires specific and well-guarded facilities for radiation. Hormone therapy is still quite costly, and androgen-independent prostate cancers arise frequently after continuous application of hormone therapy for a long period of time.[23] Establishment of safe and affordable therapies is therefore awaited.

Polyethylene glycol (PEG) has long been utilized to fuse different types of cells, as described above. Various cancer cells have been demonstrated to become fused by high concentrations (30–50%) of PEG.[24] We investigated whether the induction of apoptosis in cancer cells could result from such multinucleated cell formation as multinucleated cells induced by various cell-damaging agents, such as irradiation, doxorubicin, and docetaxel, have been shown to cause cell death by apoptosis.[25–27] We treated PC-3 cells under various conditions *in vitro* with PEG 1000 (refered to hereafter as 'PEG'). Interestingly, a concentration of PEG as low as 0.5–1.0% efficiently induced multinucleated cells under conditions of high cell density, and induced apoptosis after 34–38 h *in vitro*. PEG treatment at a low cell density ('ordinary culture conditions') was not similarly effective. When 0.5% PEG in phosphate-buffered saline (PBS) was injected directly into PC-3 xenografts in nude mice, tumor

[4]To whom correspondence should be addressed.
E-mail: hnakagam@gan2.res.ncc.go.jp

doi: 10.1111/j.1349-7006.2008.00781.x

growth was suppressed substantially compared to the PBS-injected control group. The potential molecular mechanisms underlying the suppressive effects of PEG on cell proliferation both *in vitro* and *in vivo* are discussed.

Materials and Methods

Chemicals. PEG and dimethylsulfoxide were obtained from Merck (Darmstadt, Germany), propidium iodide (PI), and etoposide were from Sigma (St Louis, MO, USA) and RNase A was from Qiagen (Valencia, CA, USA). DNA ladders of 100 bp (New England Biolabs, Beverly, MA, USA) and 1 kb (Promega, Madison, WI, USA) were used as molecular weight markers.

Cell culture. PC-3 cells were purchased from the American Type Culture Collection (ATCC; Manassas, VA, USA) and cultured at 37°C in Dulbecco's modified Eagle's medium (DMEM; Invitrogen Life Technologies, Carlsbad, CA, USA) supplemented with 10% heat-inactivated fetal bovine serum (FBS; Invitrogen Life Technologies), penicillin (100 U/mL), and streptomycin (50 U/mL) (Invitrogen Life Technologies) under a humidified atmosphere with 5% CO_2. DMEM (without FBS) was also used to make serial dilutions of PEG before addition into cell culture media.

Polyethylene glycol treatment protocol. PC-3 cells (1×10^6) were suspended in 100 μL of 0.5 and 1.0% PEG in DMEM (without FBS), incubated at room temperature for 1, 5, 15, or 30 min, then diluted 1:10 with DMEM and incubated at room temperature for 10 min. The cells were collected by centrifugation, gently washed twice with PBS, suspended in 10 mL of culture medium with FBS, seeded into 100-mm culture dishes with cover glasses at the bottom, and propagated for 34, 36, and 38 h. Cover glasses were then removed, the adherent cells on the cover glasses were fixed with 100% ethanol for 15 min, stained with PI solution (50 μg PI and 100 μg RNase A in 1.0 mL PBS), and then counted using a microscope. We adopted the criterion that cells having two or more nuclei were multinucleated. More than 500 cells within a randomly selected area on cover glasses were counted, and the cell counting was repeated three times for each experimental group.

Cell-growth assay. The effect of PEG on PC-3 cell growth was then evaluated under two different conditions. In the first condition, PC-3 cells (5×10^3) were plated in 100-mm culture dishes and incubated overnight ('ordinary culture conditions'). Aliquots of PEG in DMEM (1.0 mL) were added directly to cell culture dishes to give a final concentration of 0.5 or 1.0%, and the cells were propagated on the plates. As a reference control, 1.0 mL DMEM alone was added to the culture plates. The cells were harvested at 24, 36, 48, and 72 h after the addition of PEG, stained with trypan blue, and viable cell numbers were counted at each time point. Alternatively, 5×10^3 cells were treated following the PEG treatment protocol with 0, 0.5, or 1.0% PEG, seeded and propagated as above. In this case, cells were exposed to PEG for 1, 5, 15, and 30 min. Cells were then seeded in culture plates, propagated and harvested at 24, 36, 48, and 72 h after PEG treatment, including the nonadherent cells.

Detection of nuclear condensation. PC-3 cells were treated with 1.0% PEG for 30 min following the PEG treatment protocol, and seeded in 100-mm plates. Cells were collected after 34 h, fixed with 1.0% glutaraldehyde in PBS, incubated at 4°C overnight, collected by centrifugation, and resuspended in 50 μL PBS. After mixing thoroughly, 2 μL Hoechst 33258 (Dojindo, Kumamoto, Japan) was added to visualize nuclear condensation.

Poly(ADP-ribose) polymerase-1 cleavage. PC-3 cells were exposed to 0, 0.5, 1.0, or 2.0 PEG for 30 min, as described above. Cells were collected after 34 h and suspended in lysis buffer (50 mM Tris-HCl [pH 7.4], 150 mM NaCl, 1.0% Triton X-100) containing a protease inhibitor cocktail (Complete Mini; Roche, Indianapolis, IN, USA). Whole-cell lysates were electrophoresed on 5–20% linear gradient Tris-HCl-ready gels (Bio-Rad, Hercules, CA, USA) and fractionated proteins were transferred to polyvinylidene fluoride membranes (Immobilon-P; Millipore, Billerica, MA, USA). Western blot analysis was then carried out, as described elsewhere,[28] with mouse monoclonal antibody (mAb) against poly(ADP-ribose) polymerase (PARP)-1 (C2-10, 1:1000; Oncogene Research Products, San Diego, CA, USA) and mouse mAb against glyceraldehyde 3-phosphatase dehydrogenase (1:5000; Chemicon International, Temecula, CA, USA) as primary antibodies. For the secondary antibodies, horseradish peroxidase-conjugated antibodies against mouse IgG (NA9310V, 1:5000; Amersham Biosciences, Piscataway, NJ, USA) were used. Immunoreactive bands on the blots were visualized with chemiluminescence substrates (Immobilon Western; Millipore, Billerica, MA, USA). As a positive control, lysates were used from cells treated with a topoisomerase II inhibitor etoposide, which is known to induce apoptosis. Etoposide was dissolved in dimethylsulfoxide (25 mg/mL) and added to culture media to give a final concentration of 25 μg/mL.[29,30] Quantification of the cleaved PARP-1 protein was carried out using MultiGauge software (Fujifilm, Tokyo, Japan). Western blot analysis was carried out at least in triplicate.

Detection of DNA fragmentation. Following the PEG treatment protocol, PC-3 cells were exposed to 0, 0.5, 1.0, or 2.0% PEG for 30 min, seeded in 100-mm culture plates, and propagated for up to 38 h. Cells were collected, and DNA was extracted using a DNeasy Blood & Tissue Kit (Qiagen) following the manufacturer's instructions. Aliquots of extracted DNA samples were fractionated on a 1.5% SeaKem GTG agarose gel (Cambrex, Bio Science Rockland, Rockland, ME, USA). A DNA sample extracted from PC-3 cells treated with etoposide (25 μg/mL) for 48 h was used as a positive control.

Quantification of apoptosis by flow cytometry. PC-3 cells were treated with 0.5 or 1.0% PEG for 1 min following the PEG treatment protocol, seeded in 100-mm culture dishes and propagated in DMEM media without PEG for 36 h. Cells were harvested, washed gently with PBS, collected by centrifugation, and then stained using a MEBCYTO Apoptosis Kit (MBL, Nagoya, Japan) following the manufacturer's instructions. Cells were doubly stained with Annexin-V and PI, and the fluorescence intensities were measured by flow cytometry (FCM) (FACScan; BD Bioscience, San Jose, CA, USA) using the CellQuest analysis program.[31] We also conducted FCM analyses as above to evaluate the populations of apoptotic cells specifically among the large cells. Briefly, fluorescence intensities of the PI signal in DMEM-treated PC-3 cells were extracted from FCM data sets, expressed using FL-2A (representing DNA content) and FL-2W (representing cell size), and gated by the R1 region (representing the large-cell population), the cut-off value for which was set arbitrarily. The same scale was applied to the 0.5% PEG-treated cells. Cells extracted by the R1 region were replotted by PI signals against Annexin-V.

Cell cycle analyses by FCM. Following the PEG treatment protocol, PC-3 cells were exposed to 0, 0.5, 1.0, 2.0, or 10% PEG for 1 min, seeded in 100-mm culture plates, and propagated for 24, 34, 36, and 38 h. Cells were collected, fixed with 100% cold ethanol, and kept at –20°C overnight. After centrifugation, cells were resuspended in PI solution, incubated at room temperature for 15 min, and passed through nylon mesh (Becton, Dickinson and Company, Franklin Lakes, NJ, USA). The fluorescence intensities of PI were measured by FCM using a total of 20 000 PC-3 cells, and the number of cells in the sub-G_1, G_1, S, G_2/M, and >G_2/M (the population of cells with DNA contents beyond the G_2/M peak) fractions was counted at 24–38 h after PEG treatment. We further examined the number of PC-3 cells in large-cell populations and aneuploid populations using the same FCM data sets above at 34 and 36 h after PEG treatment.

doi: 10.1111/j.1349-7006.2008.00781.x

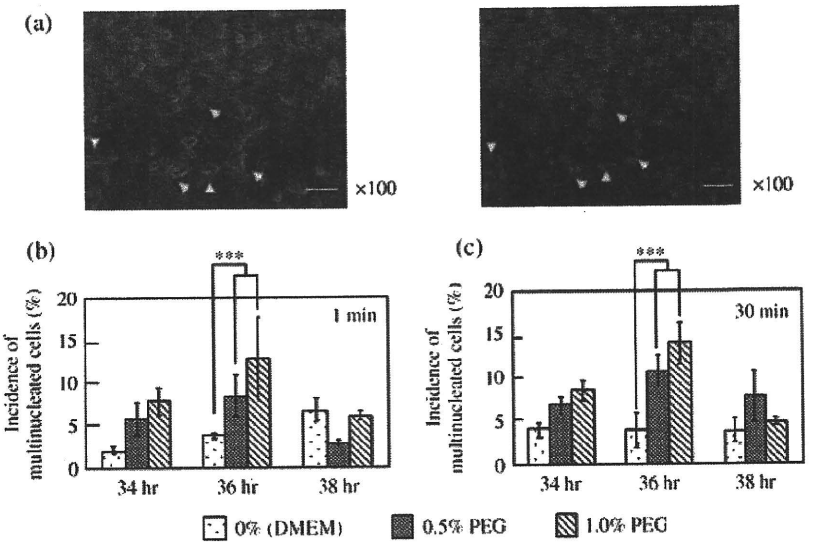

Fig. 1. Polyethylene glycol (PEG) induces multinucleated cells. (a) Following the PEG treatment protocol, PC-3 cells were treated with 0.5% PEG for 30 min. Cells were stained with propidium iodide (PI) (red). The left panel indicates the morphological features of the PEG-treated cells under microscopic observation with a green filter. The right panel indicates the nuclear staining of cells with PI. Both panels are the same magnification. The arrows indicate typical multinucleated cells. Scale bars = 50 μm. (b,c) Incidences of multinucleated cells in a total of 500 cells treated with PEG for (b) 1 min and (c) 30 min are shown. Values are the mean of fold ± SD. ***Differences of cell number between PEG treatment (0.5 and 1.0%) and the Dulbecco's modified Eagle's medium (DMEM)-treated control ($P < 0.001$).

Effects of PEG on in vivo tumor growth. The effect of PEG on PC-3 xenograft tumor growth was evaluated under two different conditions *in vivo*. With one of these, following the PEG treatment protocol, PC-3 cells (5×10^6 cells) were pretreated with DMEM or 0.5% PEG for 30 min, and then treated cells were implanted subcutaneously into the backs of BALB/c-nu/nu male mice (CLEA, Tokyo, Japan). Alternatively, PC-3 cells (5×10^6) were first implanted subcutaneously into the back of each mouse, and then at day 7 after implantation, 200-μL aliquots of PBS alone or 0.5% PEG solution in PBS were injected directly into the tumors using a 25-gauge injection needle (Terumo Corporation, Tokyo, Japan). Thereafter, tumors were measured twice a week throughout the experimental period of 19 days, and tumor volume was calculated using the following formula: (length [mm]) × (width [mm])^2 × 0.52. In these experiments, a total of 16 nude mice was randomly separated into four groups (4 × 4) receiving: DMEM treatment; 0.5% PEG treatment; intratumor PBS injection; and intratumor 0.5% PEG injection. PC-3 cells were implanted at two sites for each mouse. Animal experimental protocols were approved by the Committee for Ethics in Animal Experimentation, and the experiments were conducted in accordance with the guidelines for Animal Experiments of the National Cancer Center (Tokyo, Japan).

Histopathological analysis and detection of apoptosis in PC-3 xenografts. PC-3 xenografts were extirpated at 36–38 h after the last injection of PBS or 0.5% PEG for fixation in 10% neutralized formalin and embedding in paraffin blocks. Serial sections were prepared at 3.5-μm thickness, stained with hematoxylin and eosin (H&E), and subjected to histopathological analysis by a trained pathologist (M. W.). Apoptotic cells were detected using the TdT-mediated dUTP-biotin nick end-labeling (TUNEL) method,[32] which was carried out *in situ* using the DeadEnd Colorimetric TUNEL System (Promega) following the manufacturer's protocol.

Statistical analysis. All statistical analyses were carried out with Wilcoxon signed-ranks test using KaleidaGraph software (Synergy Software, Reading, PA, USA). Differences were considered significant when the P-value was less than 0.05.

Results

Induction of multinucleated PC-3 cells by PEG treatment *in vitro*. With the PEG treatment protocol, higher numbers of multinucleated cells were observed after PEG treatment, using 0.5–1.0% PEG (Fig. 1a). The incidence of multinucleated cells peaked at 36 h, being 8.4 and 13% with 0.5 and 1.0% PEG, respectively (Fig. 1b). The incidence only slightly increased with a longer exposure to PEG for 30 min (Fig. 1c).

Effects of PEG on PC-3 cell growth *in vitro*. In order to exclude possible toxic effects of PEG on PC-3 cells, we cultured PC-3 cells under two different culture conditions. When PC-3 cells were propagated under ordinary culture plates, and PEG was added into the media, no significant effect on cell growth was observed up to 72 h in the presence of 0.5 and 1.0% PEG, compared with the non-PEG treated control (Fig. 2a). However, significant differences were observed in cell growth between PEG-treated and DMEM-treated control cells when PC-3 cells were treated with 0.5% PEG (Fig. 2b) and 1.0% PEG (Fig. 2c) at a high cell density for 5–30 min, as in the PEG treatment protocol. A decrease in cell numbers became most prominent at around 36 h after PEG treatment (Fig. 2b,c).

Biochemical analyses for apoptosis. We observed nuclear condensation in multinucleated PC-3 cells on staining with Hoechst 33258 (Fig. 3a), suggesting induction of apoptosis.[33] Although DNA ladder formation was not observed in PEG-treated PC-3 cells, DNA samples extracted from the cells treated with PEG were substantially degraded compared to the DMEM-treated control (data not shown). Furthermore, PARP-1 cleavage, another characteristic feature of apoptosis,[34] was demonstrated in a PEG dose-dependent manner (Fig. 3b). The ratio of cleaved PARP-1 was increased by 14–52% in PEG-treated PC-3 cells when compared to the DMEM-treated control cells, although the increase was not so drastic (Fig. 3c).

Quantification of apoptosis by FCM. FCM analysis by double staining with Annexin-V (horizontal axis) and PI (vertical axis) demonstrated substantial induction of apoptosis, as depicted in Figure 4a. The incidence of cells in the early apoptotic phase (Annexin-V$^+$, PI$^-$) was 16.3%, and that in late apoptotic phase (Annexin-V$^+$, PI$^+$) was 9.2% after treatment with 0.5% PEG (Fig. 4a right). An approximate 10-fold increase was observed in the percentage of Annexin-V-positive cells (25.5%) with PEG treatment compared to 2.8% for the DMEM-treated control (Fig. 4a left). Furthermore, multinucleated cells demonstrated positive staining for Annexin-V (arrows in Fig. 4b).

In order to clarify whether apoptosis was induced mainly in multinucleated cells, we extracted FCM data sets of only large cells (Fig. 5a), and then replotted the PI signals of each cell against the Annexin-V signals using the above data (Fig. 5b). In Figure 5a, the number of cells in the large-cell fraction (R1), the cut-off value for which was set arbitrarily, increased almost three-fold (8.52 vs 24.26% among 10 000 cells analyzed) after

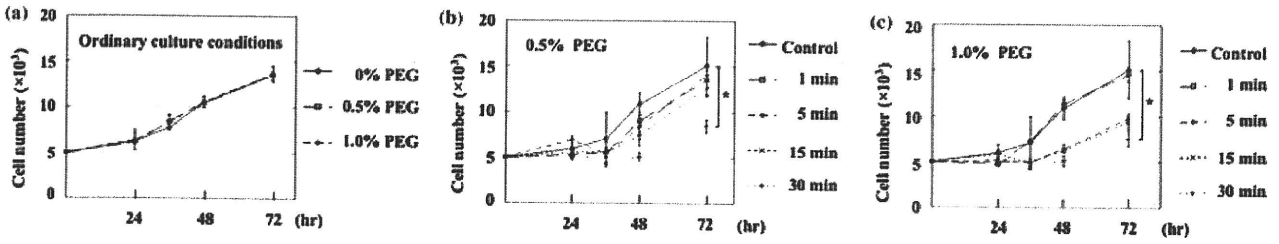

Fig. 2. Polyethylene glycol (PEG) suppresses cell growth at a high cell density. (a) After PEG solution was added into culture media, viable PC-3 cells were counted. (b,c) Following the PEG treatment protocol, PC-3 cells were treated with (b) 0.5% or (c) 1.0% PEG for 1, 5, 15, and 30 min, and viable cells were counted. Values are the mean of fold ± SD. (b) Differences of cell number between 0.5% PEG (30 min) and the Dulbecco's modified Eagle's medium (DMEM)-treated control, and (c) those between 1.0% PEG (30 min) and DMEM-treated control were significant. $^*P < 0.05$.

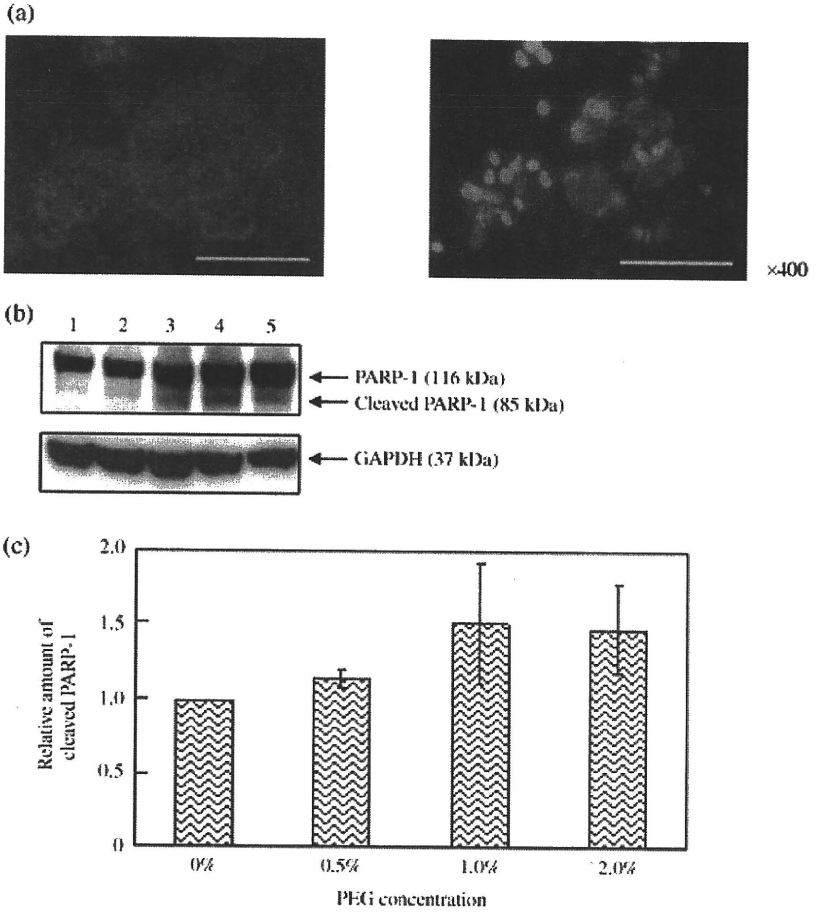

Fig. 3. DNA condensation and poly(ADP-ribose) polymerase (PARP)-1 cleavage. (a) PC-3 cells were treated with 1.0% polyethylene glycol (PEG) for 30 min following the PEG treatment protocol. Cells were stained with Hoechst 33258 (blue), as detailed in Materials and Methods. The left panel indicates the typical morphological feature of multinucleated cell (arrows). The right panel indicates the nuclear condensation of multinucleated cells. Both panels are the same magnification. Scale bars = 50 μm. (b) PARP-cleavage. Whole-cell lysates after treatment with Dulbecco's modified Eagle's medium (DMEM), PEG, or etoposide were prepared, and full-length (uncleaved) PARP-1 (116 kDa), cleaved PARP-1 (85 kDa), and glyceraldehyde-3-phosphate dehydrogenase (GAPDH) (37 kDa) were immunoblotted. Lane 1, DMEM; lane 2, 0.5% PEG; lane 3, 1.0% PEG; lane 4, 2.0% PEG; lane 5, etoposide (positive control). (c) Quantification of the cleaved PARP-1 protein by western blot analysis. The density of both non-cleaved and cleaved PARP-1 and of the background levels were measured, and the ratios of cleaved PARP-1 against the total PARP-1 were calculated as follows: (density of cleaved PARP-1) – (background level)/(density of total PARP-1) – (background level).

0.5% PEG treatment. In Figure 5b, among the cells in the R1 fraction, 292 and 1571 cells in DMEM-treated control and 0.5% PEG-treated group respectively, showed positive for Annexin V. Namely, an approximate five-fold increase in apoptotic cells was observed within the large-cell fraction of PEG-treated cells compared to DMEM-treated cells. In particular, a more than 20-fold increase was observed in the number of cells in early apoptotic phase (25 vs 656 cells). Similar results were obtained with various cut-off values for R1 to include 3.0% and 5.5% of total populations in DMEM-treated cells (data not shown).

No evidence of mitotic catastrophe in PEG-treated cells. By FCM analysis, no marked changes in cell cycle profile were apparent after PEG treatment (Fig. 6a). Although the number of cells in the sub-G_1 fraction was slightly increased by PEG treatment, cells in the G_1, S, G_2/M, and > G_2/M fractions were not changed significantly (Fig. 6b). We also noted that the number of cells in > G_2/M fractions decreased substantially between 34 and 36 h after PEG treatment, as depicted in Supplemental Fig. 1.

We then extracted aneuploid-cell and large-cell populations from the > G_2/M fraction using the FCM data set, as detailed in Supplemental Fig. 2A, and the corresponding number of cells in Supplemental Fig. 2A was counted between 34 and 36 h (Supplemental Fig. 2B). The number of aneuploid cells in the > G_2/M fraction did not show a significant change between 34 and 36 h after 0.5 and 1.0% PEG treatment. However, an approximate 20% increase in the numbers of large cells in the > G_2/M fraction was observed 34 h after PEG treatment, which substantially decreased at 36 h (Supplemental Fig. 2B). These results further

doi: 10.1111/j.1349-7006.2008.00781.x

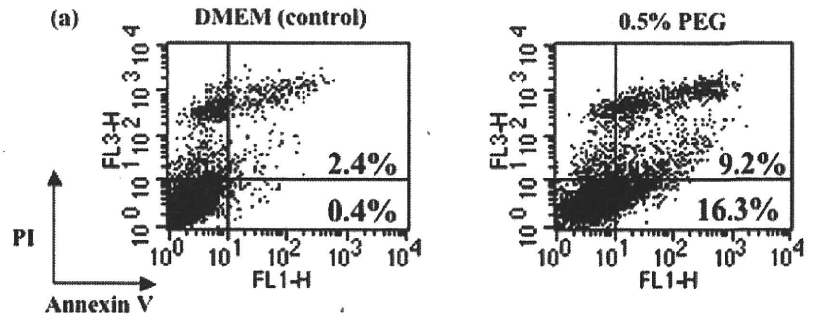

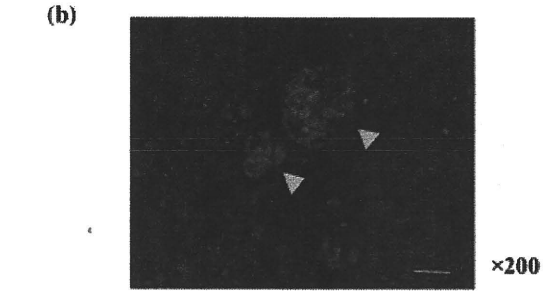

Fig. 4. Quantification of apoptosis using flow cytometry (FCM). (a) PC-3 cells were treated with Dulbecco's modified Eagle's medium (DMEM) alone (left) or 0.5% polyethylene glycol (PEG) (right) for 1 min following the PEG treatment protocol. After double-staining with Annexin-V and propidium iodide (PI), apoptotic cells were analyzed by FCM. (b) Multinucleated giant cells (arrow) visualized by staining with Annexin-V (green) and PI (red). Scale bar = 50 μm.

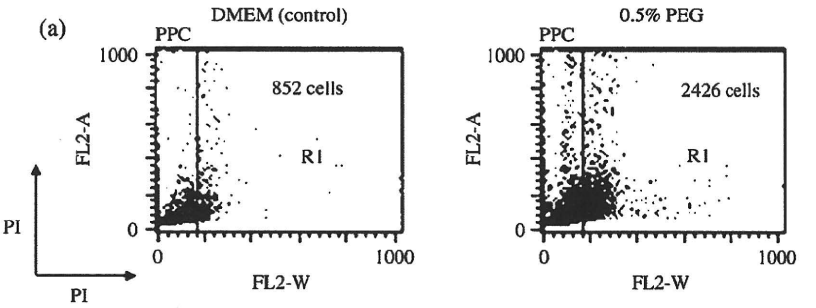

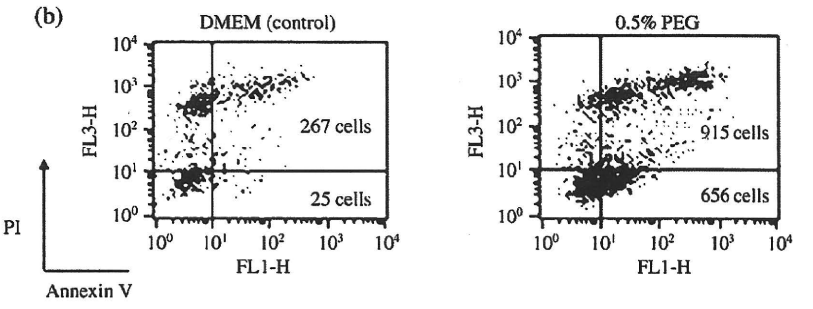

Fig. 5. Induction of apoptosis in large cells induced by polyethylene glycol (PEG) treatment. (a) From the data sets presented in Figure 4a, large cell populations were examined. (b) On the data sets presented in (a), the large cells gating the R1 region were replotted by propidium iodide (PI) signals against Annexin-V.

support the view that reduction of cell numbers by PEG treatment occurs in large-cell fractions, possibly by apoptosis, but not by mitotic catastrophe in aneuploid cells.

Induction of apoptosis by PEG in PC-3 xenografts. Following the PEG treatment protocol, PC-3 cells were pretreated with DMEM or 0.5% PEG and then implanted into mice. At day 7, the tumor volume of the PEG-treated group was significantly reduced compared to the DMEM-treated group. An approximate 50% reduction in tumor volume was observed with PEG treatment (Fig. 7a). To further confirm the growth-suppressive effect of PEG in an *in vivo* setting, we conducted the following experiment. Non-treated PC-3 cells were implanted into mice, and PBS or 0.5% PEG solution was injected into palpable tumors from day 7, twice a week (Fig. 7b top). The volumes of PC-3 xenografts increased approximately eight-fold from day 7 to day 25 in the PBS-injected group (Fig. 7b bottom). In contrast, substantial suppression of tumor growth was detected after injecting 0.5% PEG solution directly into tumors. The average sizes of tumors in PBS- and 0.5% PEG-injected groups at day 25 were 1344 ± 292 and 812 ± 215 mm^3, respectively. Namely, tumor volumes were reduced approximately 30% in the PEG-injected group compared with those in the PBS group at

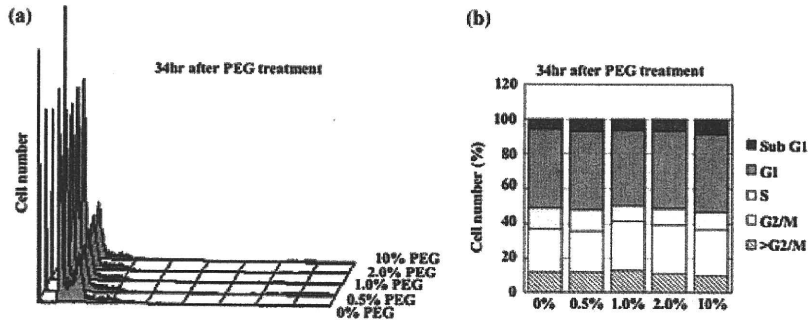

Fig. 6. Cell cycle analysis. (a) Cell cycle profiles after polyethylene glycol (PEG) treatment at 34 h are demonstrated. (b) From the data sets presented in (a), the cell population of each fraction (sub-G_1, G_1, S, G_2/M, and > G_2/M fraction) in the cell cycle is shown.

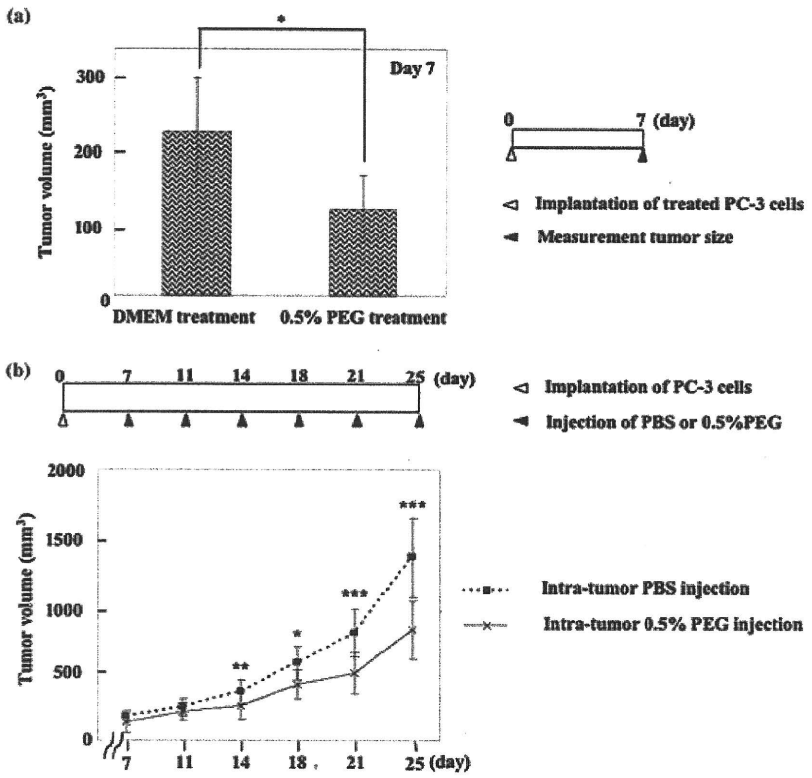

Fig. 7. Growth-suppressive effects of 0.5% polyethylene glycol (PEG) on PC-3 xenografts in nude mice. (a) After PC-3 cells were treated with Dulbecco's modified Eagle's medium (DMEM) or 0.5% PEG for 30 min, the cells were implanted into the backs of nude mice at day 0. Tumor volumes were measured at day 7. (b) Experimental protocols. PC-3 cells were implanted into backs of nude mice at day 0, and then 200 μL aliquots of phosphate-buffered saline (PBS) or 0.5% PEG was injected into palpable tumors twice a week during 19 days (top). Growth curves on PC-3 xenografts injected with PBS (■) or 0.5% PEG (X) are demonstrated (bottom). Values are the mean of fold ± SD. $*P < 0.05$, $**P < 0.01$, $***P < 0.001$.

day 25 (Fig. 7b bottom). No significant change in bodyweight was observed between the two groups during the experimental period (data not shown). Histopathological analysis revealed the presence of vacant spaces in tumors at the site of injection (Fig. 8a–d). Multinucleated cells were frequently observed surrounding these spaces in PEG-injected groups, and multinucleated cells were observed in approximately 20% of the total TUNEL-positive cells. In contrast, few TUNEL-positive cells were detected in PBS-injected tumors, although necrotic lesions were similarly observed. Multinucleated cells were rarely apparent in PBS-injected tumors (Fig. 8c,e).

Discussion

The present study demonstrated the antitumor effects of PEG via multinucleated cell formation, presumably though the induction of cell fusion. This is in line with the recent report by Roy *et al.* that PEG 800 induces apoptosis in two human colonic adenocarcinoma cells, HT29 and CaCo-2, at concentrations of 3.6–4.8%.[35] Although they briefly described PEG-induced cell fusion to be a possible mechanism, they considered this unlikely because a much higher concentration of PEG, around 30–50%, is generally required to induce cell fusion.[35]

In the present study, we were indeed able to demonstrate that low concentrations of PEG could induce apoptosis via multinucleated cell formation. More surprisingly, nuclear condensation was evident in a fraction of the multinucleated cells. As it has been reported that the cell-fusion process occurs within 1–2 h, mitotic catastrophe should be considered as a causative event for the induction of cell death by PEG.[36] However, the number of aneuploid cells in the > G_2/M fraction did not show a significant change during this time, and the number of large multinucleated cells decreased between 34 and 36 h. Therefore, an abrupt decrease in cell numbers after PEG treatment of PC-3 cells *in vitro* is reasonably explained by the induction of apoptosis in multinucleated cells, although clumped cells with aneuploid

doi: 10.1111/j.1349-7006.2008.00781.x

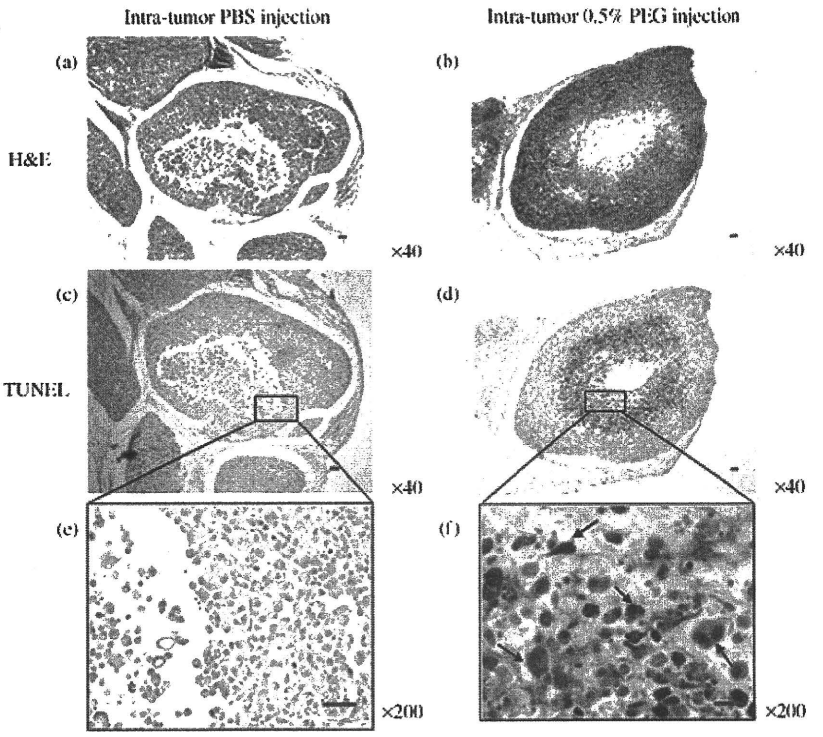

Fig. 8. Induction of multinucleated cells and apoptosis by polyethylene glycol (PEG) injection in PC-3 xenografts. Tumors with similar sizes were selected and allotted randomly into two groups. Aliquots (200 μL) of phosphate-buffered saline (PBS) or 0.5% PEG were injected directly into each group of tumors at days 7, 11, 14, 18, 21, and 25. Representative histological features of tumors in experimental groups of (a,c,e) PBS injection and (b,d,f) PEG injection are presented. The tumor sizes at day 7 before the PBS and 0.5% PEG injections were 180 ± 42 and 140 ± 70 mm^3, respectively. (a,b) Hematoxylin and eosin (H&E) staining. (c–f) TdT-mediated dUTP-biotin nick end-labeling (TUNEL) immunohistochemical staining. (e,f) Magnified images of (c) and (d), respectively. The arrows indicate typical multinucleated cells positive for TUNEL staining. Scale bars = 50 μm.

characteristics may also be a part of the large-cell fraction. Further work is needed to substantiate this possibility, but the positive staining for Annexin-V and PI and PARP-1 cleavage provide some support for this hypothesis.

Taking the results together, it is plausible that multinucleated cell formation is a trigger and causative event for the induction of apoptosis by PEG. Although an increase in osmotic pressure by PEG has been considered to be important for its cytostatic or apoptotic effects,[35] it is unlikely that osmotic pressure played a role with the low concentrations of PEG used here. Indeed, when PC-3 cells were cultured in the presence of PEG under ordinary culture conditions, we did not detect apparent changes in cell-growth properties for up to 72 h (Fig. 2a). This negates the possible implication of osmotic pressure in the induction of apoptosis by the concentrations of PEG used in the present conditions. Another possibility to be considered is that cell-membrane damage caused by PEG led to the induction of apoptosis. It is thought that the cell membrane could be damaged by injection of cells with PEG particles through microcylinders in *in vivo* models. Further study is warranted to corroborate or refute this point. However, the induction of nuclear condensation, positive staining for Annexin-V in multinucleated cells, and PARP-1 cleavage by PEG treatment all point to a significant role for apoptosis in the growth-suppressive effects of PEG. Although the mechanism of induction of apoptosis by PEG remains unclear, we clearly demonstrated that PEG exhibited a suppressive effect on tumor growth *in vivo* and induced apoptosis, possibly via the cell-fusion mechanism.

Lastly, we should note that PC-3 prostate cancer cells were used as a model system. The therapies for prostate cancer, for example hormone therapy or radiation therapy, have some drawbacks. Radioactive material such as iodine-125 using brachytherapy may cause chromosomal aberrations.[37] Occurrence of androgen-independent prostate cancers because of frequent or continuous application of hormone therapy is a very serious problem at present. Once cancer becomes androgen independent, metastatic lesions manifest aggressively within 12–18 months, and the average patient survival time is only 2–3 years.[38] Although chemotherapies have been adapted for androgen-independent aggressive cancer cases, the tumor-suppressive effects brought about by those therapies are not satisfactory.[39] Therefore, for cases with localized non-invasive lesions, urologists generally choose radical prostatectomy.[40] At the same time, however, there are a substantial number of cases in which radical therapy cannot be conducted because of the poor compliance of patients and life-threatening side effects.[41,42]

In the present study, we clearly demonstrated that PEG is able to induce apoptosis in PC-3 cells in an autonomous cell-fusion manner, with efficient suppression of tumor growth *in vivo*. Based on our observations, we propose that direct intratumoral injection of PEG could be a promising therapeutic approach for androgen-independent prostate cancers. Clearly, if PEG is injected in clinical trials, it may induce cell fusion for normal prostate cells, and unwanted side effects may appear. However, even if PEG induces multinucleated cells between normal and tumor cells, it could be effective for diffuse types of prostate cancer. In addition, direct intratumoral injection of PEG could also assist hormone therapy and radiation therapy. Although several problems remain to be solved, the potential of PEG as a novel, non-invasive and non-toxic therapeutic agent clearly warrants further attention.

Acknowledgments

The authors thank Masako Ochiai and Ibuki Kobayashi (Biochemistry Division, National Cancer Center Research Institute) for technical help and discussion throughout this study. This work was supported in part by a Grant-in-Aid for the Third-Term Comprehensive 10-Year Strategy for Cancer Control from the Ministry of Health, Labour, and Welfare of Japan, and in part by a Grant-in-Aid for Cancer Research from the Ministry of Health, Labour, and Welfare of Japan. K. F. was a recipient of a Research Resident Fellowship from the Foundation for Promotion of Cancer Research in Japan during the research.

References

1 Schiller LR, Emmett M, Santa Ana CA, Fordtran JS. Osmotic effects of polyethylene glycol. *Gastroenterology* 1988; **94**: 933–41.
2 Elsenhans B, Caspary WF. Differential changes in the urinary excretion of two orally administered polyethylene glycol markers (PEG 900 and PEG 4000) in rats after feeding various carbohydrate gelling agents. *J Nutr* 1989; **119**: 380–7.
3 Hunnuksela M, Pirila V, Salo OP. Skin reactions to propylene glycol. *Contact Dermatitis* 1975; **1**: 112–16.
4 Ramkumar D, Rao SS. Efficacy and safety of traditional medical therapies for chronic constipation: systematic review. *Am J Gastroenterol* 2005; **100**: 936–71.
5 Quartier S, Garmyn M, Becart S, Goossens A. Allergic contact dermatitis to copolymers in cosmetics – case report and review of the literature. *Contact Dermatitis* 2006; **55**: 257–67.
6 Veronese FM, Pasut G. PEGylation, successful approach to drug delivery. *Drug Discov Today* 2005; **10**: 1451–8.
7 Molineux G. Pegylation: engineering improved pharmaceuticals for enhanced therapy. *Cancer Treat Rev* 2002; **28**: 13–16.
8 Rassoulzadegan M, Binetruy B, Cuzin F. High frequency of gene transfer after fusion between bacteria and eukaryotic cells. *Nature* 1982; **295**: 257–9.
9 Chiu DT. A microfluidics platform for cell fusion. *Curr Opin Chem Biol* 2001; **5**: 609–12.
10 Naigamwalla D, Chia MC, Tran TT *et al.* Polyethylene glycol 8000 and colon carcinogenesis: inhibition in the F344 rat, promotion in the Min mouse. *Cancer Res* 2000; **60**: 6856–8.
11 Corpet DE, Parnaud G, Delverdier M, Peiffer G, Tache S. Consistent and fast inhibition of colon carcinogenesis by polyethylene glycol in mice and rats given various carcinogens. *Cancer Res* 2000; **60**: 3160–4.
12 Nakagama H, Nakanishi M, Ochiai M. Modeling human colon cancer in rodents using a food-borne carcinogen, PhIP. *Cancer Sci* 2005; **96**: 627–36.
13 Klurfeld DM. Dietary fiber-mediated mechanisms in carcinogenesis. *Cancer Res* 1992; **52**: 2055S–9S.
14 Parnaud G, Tache S, Peiffer G, Corpet DE. Polyethylene-glycol suppresses colon cancer and causes dose-dependent regression of azoxymethane-induced aberrant crypt foci in rats. *Cancer Res* 1999; **59**: 5143–7.
15 Roy HK, Gulizia J, DiBaise JK *et al.* Polyethylene glycol inhibits intestinal neoplasia and induces epithelial apoptosis in Apc (min) mice. *Cancer Lett* 2004; **215**: 35–42.
16 Webber MM, Bello D, Quader S. Immortalized and tumorigenic adult human prostatic epithelial cell lines. characteristics and applications. Part I. Cell markers and immortalized nontumorigenic cell lines. *Prostate* 1996; **29**: 386–94.
17 Ahmedin J, Rebecca S, Elizabeth W, Taylor M, Jiaquan X, Michael JT. Cancer statistics, 2007. *CA Cancer J Clin* 2007; **57**: 43–66.
18 Marugame T, Mizuno S. Comparison of prostate cancer mortality in five countries. France, Italy, Japan, UK and USA from the WHO mortality database (1960–2000). *Jpn J Clin Oncol* 2005; **35**: 690–1.
19 Huggins C, Hodges CV. Studies on prostate cancer: effect of castration, estrogen and androgen injection on serum phosphatases in metastatic carcinoma of the prostate. *Cancer Res* 1941; **1**: 293–7.
20 Singh P, Uzgare A, Litvinov I, Denmeade SR, Isaacs JT. Combinatorial androgen receptor targeted therapy for prostate cancer. *Endocr Relat Cancer* 2006; **13**: 653–66.
21 Di Lorenzo G, Autorino R, Figg WD, De Placido S. Hormone-refractory prostate cancer: where are we going? *Drugs* 2007; **67**: 1109–24.
22 Randy VH. Modern brachytherapy for treatment of prostate cancer. *Cancer Control* 2007; **14**: 238–43.
23 Scher HI, Kelly WK. Flutamide withdrawal syndrome: its impact on clinical trials in hormone-refractory prostate cancer. *J Clin Oncol* 1993; **11**: 1566–72.
24 Laboisse CL, Maoret JJ, Triadou N, Augeron C. Restoration by polyethylene glycol of characteristics of intestinal differentiation in subpopulations of the human colonic adenocarcinoma cell line HT29. *Cancer Res* 1988; **48**: 2498–504.
25 Bindu L, Balaram P, Mathew A, Remani P, Bhattathiri VN, Nair MK. Radiation-induced changes in oral carcinoma cells – a multiparametric evaluation. *Cytopathology* 2003; **14**: 287–93.
26 Liu MJ, Wang Z, Ju Y, Zhou JB, Wang Y, Wong RN. The mitotic-arresting and apoptosis-inducing effects of diosgenyl saponins on human leukemia cell lines. *Biol Pharm Bull* 2004; **27**: 1059–65.
27 Makarovskiy AN, Siryaporn E, Hixson DC, Akerley W. Survival of docetaxel-resistant prostate cancer cells *in vitro* depends on phenotype alterations and continuity of drug exposure. *Cell Mol Life Sci* 2002; **59**: 1198–211.
28 Tsuchiya N, Fukuda H, Sugimura T, Nagao M, Nakagama H. LRP130, a protein containing nine pentatricopeptide repeat motifs, interacts with a single-stranded cytosine-rich sequence of mouse hypervariable minisatellite Pc-1. *Eur J Biochem* 2002; **269**: 2927–33.
29 Shimada K, Nakamura M, Ishida E, Kishi M, Yonehara S, Konishi N. c-Jun NH2-terminal kinase-dependent Fas activation contributes to etoposide-induced apoptosis in p53-mutated prostate cancer cells. *Prostate* 2003; **55**: 265–80.
30 Obasaju C, Hudes GR. Paclitaxel and docetaxel in prostate cancer. *Hematol Oncol Clin North Am* 2001; **15**: 525–45.
31 van Engeland M, Nieland LJ, Ramaekers FC, Schutte B, Reutelingsperger CP. Annexin V-affinity assay: a review on an apoptosis detection system based on phosphatidylserine exposure. *Cytometry* 1998; **31**: 1–9.
32 Gavrieli Y, Sherman Y, Ben-Sasson SA. Identification of programmed cell death *in situ* via specific labeling of nuclear DNA fragmentation. *J Cell Biol* 1992; **119**: 493–501.
33 Bedner E, Li X, Gorczyca W, Melamed MR, Darzynkiewicz Z. Analysis of apoptosis by laser scanning cytometry. *Cytometry* 1999; **35**: 181–95.
34 Soldani C, Scovassi AI. Poly (ADP-ribose) polymerase-1 cleavage during apoptosis: an update. *Apoptosis* 2002; **7**: 321–8.
35 Roy HK, DiBaise JK, Black J, Karolski WJ, Ratashak A, Ansari S. Polyethylene glycol induces apoptosis in HT-29 cells: potential mechanism for chemoprevention of colon cancer. *FEBS Lett* 2001; **496**: 143–6.
36 Lentz BR. PEG as a tool to gain insight into membrane fusion. *Eur Biophys J* 2007; **36**: 315–26.
37 Arslan NC, Geard CR, Hall EJ. Low dose-rate effects of cesium-137 and iodine-125 on cell survival, cell progression, and chromosomal alterations. *Am J Clin Oncol* 1986; **9**: 521–6.
38 Chang SS. Treatment options for hormone-refractory prostate cancer. *Rev Urol* 2007; **9**: S13–18.
39 Oh WK, Tay MH, Huang J. Is there a role for platinum chemotherapy in the treatment of patients with hormone-refractory prostate cancer? *Cancer* 2007; **109**: 477–86.
40 Freedland SJ, Moul JW. Prostate specific antigen recurrence after definitive therapy. *J Urol* 2007; **177**: 1985–91.
41 Augustin H, Hammerer P, Graefen M *et al.* Intraoperative and perioperative morbidity of contemporary radical retropubic prostatectomy in a consecutive series of 1243 patients: results of a single center between 1999 and 2002. *Eur Urol* 2003; **43**: 113–18.
42 Benoit RM, Naslund MJ, Cohen JK. Complications after radical retropubic prostatectomy in the medicare population. *Urology* 2000; **56**: 116–20.

Supplementary materials

The following supplementary material is available for this article:

Fig. S1. The cell number of > G_2/M fractions decreased between 34 and 36 h. From the data sets presented in Figure 6a, the cell number of > G_2/M fractions was counted between 24 and 38 h using flow cytometry.

Fig. S2. Disappearance of large cells between 34 and 36 h. (A) From flow cytometry data sets, the aneuploid cell (A) and large-cell (L) populations were extracted, as described elsewhere. (B) From the data sets presented in (A), each cell population was monitored between 34 and 36 h.

This material is available as part of the online article from:
http://www.blackwell-synergy.com/doi/abs/10.1111/j.1349-7006.2008.00781.x

This link will take you to the article abstract).

Please note: Blackwell Publishing are not responsible for the content or functionality of any supplementary materials supplied by the authors. Any queries (other than missing material) should be directed to the corresponding author for the article.

doi: 10.1111/j.1349-7006.2008.00781.x

Mol Cell Biochem
DOI 10.1007/s11010-008-9761-1

Hormone receptor-related gene polymorphisms and prostate cancer risk in North Indian population

Khadijeh Onsory · R. C. Sobti · Adnan Issa Al-Badran · Masatoshi Watanabe · Taizo Shiraishi · Awtar Krishan · Harsh Mohan · Pushpinder Kaur

Received: 9 October 2007 / Accepted: 7 April 2008

Abstract The purpose of this study was to analyse the frequency and type of mutations in the coding region of androgen receptor (AR) and to determine the role of polymorphisms in the intron 1 of *ERα*, exon 5 of *ERβ*, intron 7 of progesterone, exon 7 of the aromatase (*CYP19*) and exon 9 of *VDR* genes in the risk of prostate cancer. PCR-RFLP analysis of all above the genes was on 100 prostate cancer patients and an equal number of matching controls. The study also included PCR-SSCP analyses of exons 2–8 of *AR* gene. The genotype containing −/− allele of *ERα* gene was statistically significant for the risk of prostate cancer pose (OR, 2.70; 95% CI, 1.08–6.70, $P = 0.032$) Rr genotype of *ERβ* gene also have a higher risk (OR, 1.65; 95% CI, 0.52–5.23) for prostate cancer. The *Cys* allele of *CYP19* gene was also associated with statistically significant increased risk of prostate cancer (OR; 2.28, 95% CI, 1.20–4.35, $P = 0.012$). tt genotype of codon 352 of *VDR* gene showed an OR of 0.43 for (95% CI, 0.13–1.39) and an OR for Tt genotype was 0.65 (95% CI, 0.36–1.16). Taken together, the results showed that in North Indian population, *ERα* and *CYP19* genes may be playing a role in the risk of prostate cancer.

Keywords Prostate carcinoma · AR · ERs · PR · CYP19 · VDR gene polymorphisms

K. Onsory · R. C. Sobti (✉) · P. Kaur
Department of Biotechnology, Panjab University, Chandigarh 160014, India
e-mail: rcsobti@pu.ac.in

A. I. Al-Badran
Department of Biology, Basrah University, Al-Basrah, Iraq

M. Watanabe
Division of Materials Science and Chemical Engineering, Yokohama National University, Yokohama, Japan

T. Shiraishi
Second Department of Pathology, Mie University School of Medicine, Tsu, Japan

A. Krishan
Division of Radiation Oncology and Experimental Therapeutics, University of Miami Medical School, Miami, FL, USA

H. Mohan
Department of Pathology, Government Medical College, Chandigarh, India

Introduction

Epidemiological evidences have suggested that steroid hormones are involved as initiators or promoters in prostate carcinogenesis and that hormonal factors may be associated with the risk of prostate cancer [1, 2]. Androgens are required for normal male sexual development, growth, differentiation, maintenance of secondary sexual characteristics and spermatogenesis. Androgen receptor (AR) is a member of the nuclear receptor family that includes receptors for steroid and thyroid hormones, vitamin D_3 and retinoic acids, and numerous orphan receptors for which no ligands are known [3]. The AR was first described in 1969 [4] and cloned in 1988 [5]. The gene is located on the X-chromosome at Xq11–12 and spans a length of approximately 90-kb of DNA and contains eight exons [6]. The AR has been proposed as a candidate gene for several cancers (breast, prostate, uterine endometrium, colon and esophagus) [7].

Similarly, ER is expressed in a wide variety of cell types in addition to estrogen-responsive tissues such as mammary epithelium, endometrium, breast and bone. Two different *ER*s, i.e., *ERα* [8] and *ERβ* [9] have been

characterized. The human *ERα* encoding gene located on chromosome 6q24–27 consists of eight exons, seven introns, about 140 kb in length, two promoter regions and five functional domains designated A/B-F [10] result in two transcripts that differ only in the 5′ region. The protein itself has 595 amino acids with molecular weight of 66,182 Da. The *ERβ* gene is located on chromosome 14q23–24.1 [11] and consists of eight exons [12]. The DNA binding domain of *ERβ* is highly homologous to that of *ERα*, implying that both *ERα* and *ERβ* share the same DNA response element.

The human progesterone receptor gene (*HPR*) is located on chromosome 11q22–23 and its product belongs to the steroid thyroid-retinoic acid receptor superfamily of transcription factors [13]. The action of progesterone is mediated via the progesterone receptor (PR). Progesterone binds to PR and the activated PR protein translocates to the cell nucleus under the control of hinge region signals. PR–PR homodimers are formed and these interact with hormone response elements of PR-responsive genes to regulate their transcription. Thus, the cellular responses to progesterone are influenced by both PR protein level and activity of progesterone hormone levels.

Aromatase P450 is present in the endoplasmic reticulum of estrogen-reproducing cells in which it is expressed. The effects of the resulting estrogens are mediated through the estrogen receptor. The prostate $P450_{arom}$ is encoded by the *CYP19* gene localized on chromosome 15p21.1 [14] which spans at least 52 kb and contains nine coding exons beginning with exon II and an untranslated first exon (5′-termini) whose transcripts differ from one another in a tissue-specific fashion [15]. The prostate is influenced by estrogen from peripheral sources as well as through aromatase activity in its stroma [16]. Data from a prospective study suggest that the low levels of estradiol may be a risk factor for prostate cancer [17]. There is an evidence of elevated levels of aromatase activity and mRNA expression in stroma cells in prostate cancer [18], as well as increasing the evidence of cross talk between estrogens and androgens in regulating gene expression in the prostate [19]. Moreover, circulating estrogens can compete with androgens for binding to sex hormone-binding globulin, and it is generally assumed that sex hormone-binding globulin synthesis is regulated by and is a reflection of the estrogen/androgen balance [20].

Vitamin D and its metabolites are best known for their action in calcium and bone metabolism. However, epidemiological studies have suggested that an increased prostate cancer risk is associated with decreased production of vitamin D. The effects of vitamin D and its analogous are mediated by vitamin D receptor (VDR), a member of the steroid/thyroid/retinoic acid receptor superfamily, which functions as a ligand-dependent transcription factor [21]. The gene encoding VDR located on chromosome 12cen-q [22], contains 14 exons, and spans more than 75 kb of genomic DNA [23]. Bid et al. [24] determined the distribution of VDR gene (Fok-I, Taq-I and Apa-I) polymorphisms using a PCRRFLP analysis in unrelated normal healthy individuals from a north Indian population. Their results suggested that the frequency and distribution of the polymorphisms in India are substantially different from these in other populations and ethnic groups.

The genes mentioned above reveal polymorphisms and there are reports of some of them to be the risk factors for prostate cancer in populations other than India. It is, therefore, pertinent to study such polymorphisms in multiethnic Indian populations to look for genetic risk factors for prostate cancer.

Materials and methods

Patients and controls

A study group consisting of 100 prostate cancer patients were collected from the Department of Urology, Government Medical College and Hospital, Chandigarh, India. The control group consisted of 100 male healthy controls that visited Postgraduate Institute of Medical Science and Research (PGIMER) for minor treatments. All subjects were from the same ethnic group. They were asked about their age, cigarette smoking and alcohol drinking habits. Prostate cancer patients were all histologically confirmed and characterized in terms of their clinical staging (Tumour-Node-Metastasis system) and grade (Gleason score). Nine per cent (9.0%) of the patients had well differentiated, 54% moderate-differentiated and 37% poorly differentiated adenocarcinoma. Regarding clinical staging, 22% were in stage A, 15% in stage B, 23% in stage C and 40% in stage D. The informed consent was obtained from both of patients and controls.

DNA extraction

Genomic DNA of all cases and controls was isolated from either blood or frozen tissues using proteinase K digestion followed by phenol/chloroform extraction method [25] and stored at −20°C.

PCR-SSCP

The analysis of AR was based on the PCR amplification with primers given in Table 1. Amplification consisted of an initial denaturation step for 5 min at 95°C, 35 cycles of denaturation at 95°C and primer extension at 72°C for

Table 1 PCR primers for AR exons 2–8

Primers pairs	Sequence of primers	Fragment size (bp)	*AT_m (°C)
AR-2F	5′-GCC ATT CAG TGA CAT GTG TTG CAT TGG	266	60
AR-2R	5′-AAG GTT AGT GTC TCT CTC TGG AAG GT-3′		
AR-3F	5′-AAC TCA TTA TCA GGT CTA TCA ACT C-3′	243	60
AR-3R	5′-AAA ATC TGG TCT AAA GAG AGA CTA GA-3′		
AR-4F	5′-GCA TTG TGT GTT TTT GAC CAC TGA TG-3′	385	60
AR-4R	5′-GAT CCC CCT TAT CTC ATG CTC CC-3′		
AR-5F	5′-CAA CCC GTC AGT ACC CAG ACT GAC CA-3′	285	60
AR-5R	5′-AGC TTC ACT GTC ACC CCA TCA CCA TC-3′		
AR-6F	5′-CTC TGG GCT TAT TGG TAA ACT TCC-3′	294	57
AR-6R	5′-GTC CAG GAG CTG GCT TTT CCC TA-3′		
AR-7F	5′-GCT TTG TCT AAT GCT CCT TCG TGG-3′	271	60
AR-7R	5′-CTC TAT CAG GCT GTT CTC CCT GAT-3′		
AR-8F	5′-GAG GCC ACC TCC TTG TCA ACC CTG-3′	304	57
AR-8R	5′-CCA AGG CAC TGC AGA GGA GTA GTG GC-3′		

* AT_m is annealing temperature of each primer

Table 2 Distribution of allelic variants in prostate cancer patients and controls

Genotype	Cases	Controls	OR (95% CI)	*P*-value	OR (95% CI)[a]	*P*-value
+/+	28 (28%)	42 (42%)	1.00		1.00	
+/−	54 (54%)	48 (48%)	1.68 (0.91–3.12)	0.096	1.72 (0.92–3.20)	0.084
−/−	18 (18%)	10 (10%)	2.70 (1.08–6.70)	0.032	2.74 (1.10–6.84)	0.030
(+/−) + (−/−)	72 (72%)	38 (38%)	1.94 (0.86–3.23)	0.028	1.97 (1.09–3.57)	0.024
RR	92 (92%)	95 (95%)	1.00		1.00	
Rr	8 (8.0%)	5 (5.0%)	1.65 (0.52–5.23)	0.394	1.74 (0.54–5.55)	0.350
A1/A1	84 (84%)	90 (90%)	1.00		1.00	
A1/A2	16 (16%)	10 (10%)	1.71 (0.73–3.98)	0.211	1.74 (0.74–4.05)	0.200
CC	59 (59%)	73 (73%)	1.00		1.00	
CT	37 (37%)	20 (20%)	2.28 (1.20–4.35)	0.012	2.35 (1.23–4.49)	0.010
TT	4 (4.0%)	7 (7%)	0.70 (0.19–2.53)	0.594	0.70 (0.19–2.54)	0.596
CT + TT	41 (41%)	27 (27%)	1.87 (1.03–3.40)	0.038	1.91 (1.05–3.49)	0.033
TT	55 (55%)	43 (43%)	1.00		1.00	
Tt	40 (40%)	48 (48%)	0.65 (0.36–1.16)	0.147	0.66 (0.37–1.18)	0.164
tt	5 (5.0%)	9 (9.0%)	0.43 (0.13–1.39)	0.160	0.41 (0.12–1.33)	0.138
Tt + tt	45 (45%)	55 (55 %)	0.61 (0.35–1.07)	0.090	0.62 (0.35–1.08)	0.095

OR, odds ratio; CI, confidence interval

$P < 0.05$ was considered statistically significant

[a] ORs adjusted for age

1 min each. These were followed by a final elongation step for 5 min at 72°C (Figs. 1–3).

DNA sequencing

PCR products that showed normal and shifted SSCP patterns were purified directly from the PCR reaction using QIA quick PCR purification Kit (Qiagen, Germany). Their sequences were determined by cycle sequencing using ABI PRISM Big Dye Terminator Cycle Sequencing Ready Reaction Kit (Perkin-Elmer) on an automated DNA-sequencer ABI PRISM 310 (Applied Biosystems/ Perkin-Elmer).

PCR-RFLP

Estrogen receptor genotyping

The analysis of *ERα* and detection of the *PvuII* restriction endonuclease site in intron 1 was facilitated by PCR amplification of a region spanning the site with primers,

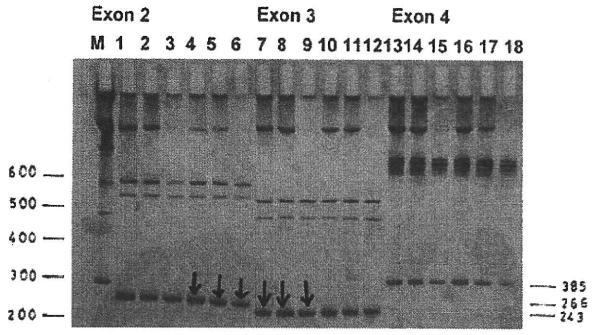

Fig. 1 DNA Silver Stained SSCP Gene Gel Excel 12.5/24 (AR gene exons 2–4). Lane M, 100 bp Marker (Invitrogen); lanes 1–6, exon 2 (266 bp); lanes 7–12, exon 3 (243 bp); lanes 13–18, exon4 (385 bp)

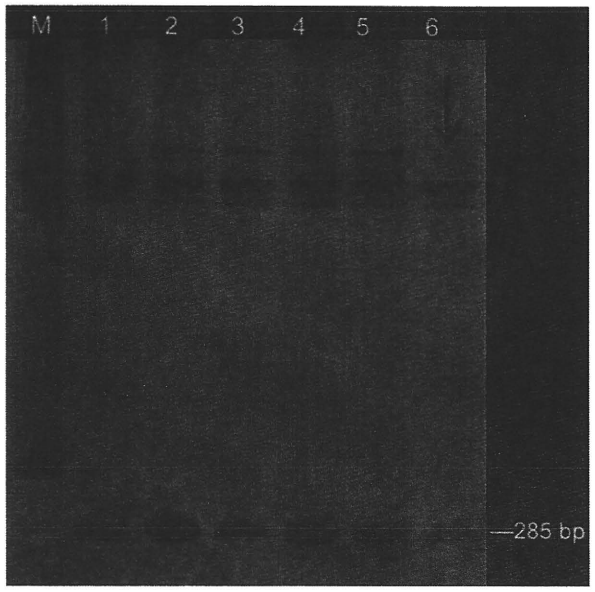

Fig. 2 PCR-SSCP analysis of *AR* gene exon 5. DNA Silver Stained SSCP Gene Gel Excel 12.5/24. Lane M, 100-bp Marker (Invitrogen); lanes 1–6, exon 5 (285-bp)

5′-ATCCAGGGTTATGTGGCAATGAC-3′ and 5′-ACCC TGGCGTCGATTATCTGA-3′. Amplification consisted of an initial 5 min denaturation at 95°C, 30 cycles of denaturation at 95°C, annealing at 57°C and elongation at 72°C for 1 min each. These were followed by a final elongation step for 5 min at 72°C. Then 10 µl aliquots of PCR products were digested with 5 units of *PvuII* restriction enzyme (New England, Biolabs, USA) followed by incubation at 37°C for 2 h. The presence of the *PvuII* restriction sites is indicated by a (+), whereas the absence of the site is denoted by a (−) (Fig. 4).

The analysis of *ERβ* was based on the PCR amplification with the primers 5′-CAGGCTTTGTGGAGCTCAG-3′ and 5′-ACCTGTCCAGAACAAGATCT-3′. Amplification consisted of an initial denaturation step for 10 min at 95°C, 30 cycle of denaturation at 95°C, annealing at 62°C and primer extension at 72°C for 1 min each. These were followed by a final elongation step for 5 min at 72°C. An aliquot 10 µl of PCR products was digested overnight at 37°C with 5 units of *RsaI* (Takara Shuzou, Kyoto, Japan) restriction endonuclease. Presence of the silent mutation in codon 328 resulted in cleavage of 144 bp PCR product with *Rsa*I restriction endonuclease into two fragments of 110 and 34 bp (Fig. 5).

Progesterone genotyping

The analysis of PROGINS was based on the PCR amplification of a fragment encompassing the 306 bp insertion polymorphism in intron 7 using the primers 5′-GCCTCTAAAATGAAAGGCAGAAAGC-3′ and 5′-GCGCGTATTTTCTTGCTAAATGTCTG-3′. Amplification was carried out for 30 cycles with denaturation at 94°C, annealing at 60°C and extension at 72°C for 1 min each. An initial denaturation step was carried out for 3 min at 94°C and a final extension for 5 at 72°C min. The A1 allele of HPR was defined as the absence of the insertion. A1 allele appeared as a 175-bp fragment and the A2 allele PROGINS appeared as a 481-bp fragment (Fig. 6).

Aromatase genotyping

PCR amplification of the coding and flanking sequence of exon 7 of the aromatase gene was carried out using the primers 5′-CGCTAGATGTCTAAACTGAG-3′ and 5′-CATATGTGGCATGGGAATTA-3′. Thermal cycling consisted of an initial 5 min denaturation step at 95°C, followed by 35 cycles of denaturation at 95°C, annealing at 51°C, elongation at 72°C for 1 min each, and a final elongation for 5 min at 72°C. Then 10 µl aliquots of the PCR products were digested at 37°C for 2 h with 5 units of *Sfa*NI (New England, Biolabs, USA) restriction enzyme. The C to T substitution in exon 7, resulting in a single amino acid substitution from Arg to Cys at codon 264, creates a recognition site for the SfaNI restriction enzyme (Fig. 8).

VDR genotyping

A 740-bp fragment encompassing the *TaqI* polymorphism site in exon 9 of *VDR* gene was amplified using primers 5′-CAGAGCATGGACAGGGAGCAA-3′ and 5′-GCAACTC CTCATGGCTGAGGTCTC-3′. Thirty-five cycles were performed using Taq polymerase with denaturation at 95°C, annealing at 64°C and extension at 72°C for 1 min each. Thereafter, 10 µl of the PCR product was subjected to restriction digestion with *TaqI* (Takara Shuzou, Kyoto, Japan) and incubated at 65°C for 3 h, and run directly on 2.0% agarose gel followed by staining with ethidium

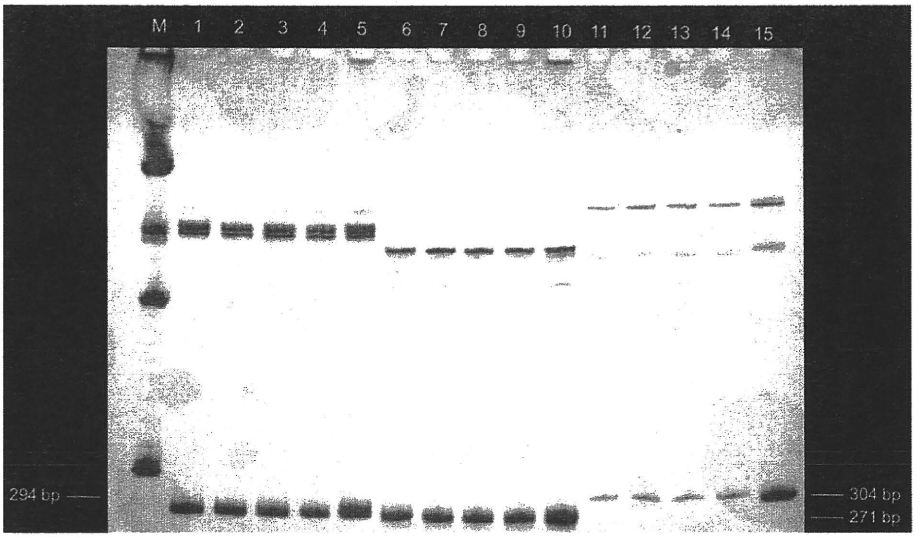

Fig. 3 DNA silver stained SSCP Gene Gel Excel 12.5/24 (AR gene exons 6–8). Lane M, 100 bp Marker (Invitrogen); lanes 1–5, exon 6 (294 bp); lanes 6–10, exon 7 (271 bp); lanes 11–15, exon 8 (304 bp)

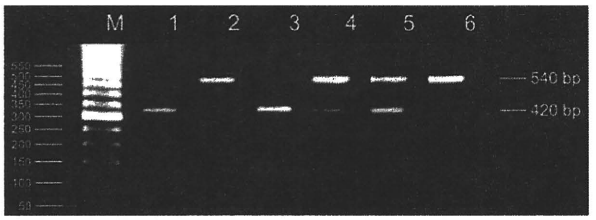

Fig. 4 RFLP-analysis of *ERa* gene using Pvull restriction enzyme. Lane M, 50-bp Marker (Invitrogen); lanes 1 and 3, +/+ (420-bp); lanes 2, 6, −/− (540-bp); lanes 4 and 5, +/− (420, 540-bp)

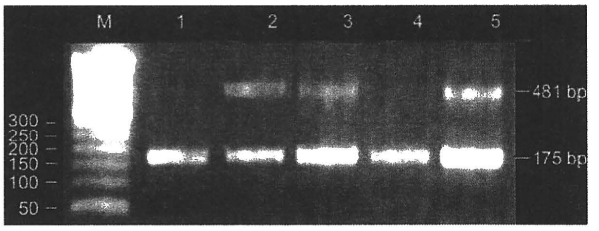

Fig. 6 PCR amplification of *PR* gene intron 7. Lane M, 50-bp Marker (Invitrogen); lanes 1, 4, A1/A1 (175-bp); lanes 2, 3, 5, A1/A2 (175, 481-bp)

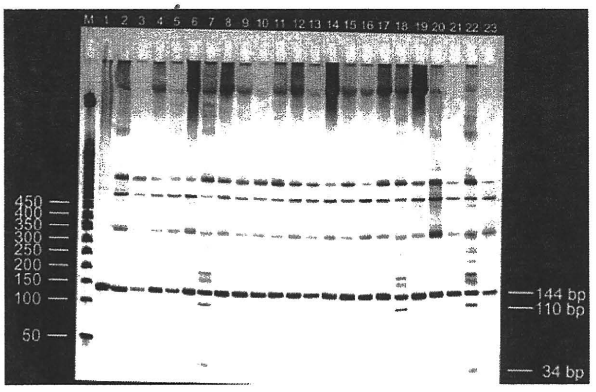

Fig. 5 RFLP analysis of ER-β gene using Rsa-I restriction enzyme. Lane M, 50 bp Marker (Invitrogen); lanes 1–6, 8–17, 19–21, 23, RR (144 bp); lane 7, 18, 22, Rr (34, 110, 144 bp)

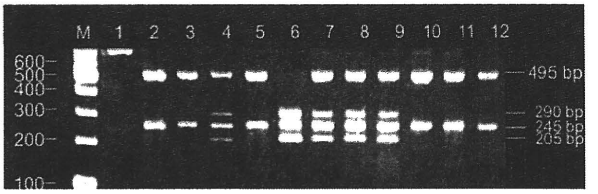

Fig. 7 RFLP-analysis of VDR gene using Taql restriction enzyme. Lanes M and 1, 100-bp marker (Invitrogen); lanes 2, 3, 5, 10–12, PCR product (740-bp); lane 6, TT (245, 495-bp), lanes 4 tt (205, 245, 290-bp); lanes 7–9 Tt (205, 245, 290, 495-bp)

bromide. The presence of C to T change at the third position of codon 352 for isoleucine in exon 9 is associated with the loss of a *TaqI* restriction site. The resulting alleles were designated T (TaqI site absent; two fragments of 495 and 245 bp) or t (TaqI site present; three fragments of 290, 245 and 205 bp). Individuals were classified as TT, Tt or tt (capital letter indicates the absence of restriction site). Amplification was performed in a final volume of 50 µl containing 40 ng of genomic DNA, 1 unit of Taq polymerase, 1.5 mM $MgCl_2$, 200 µM of each deoxynucleotide triphosphate, 0.3 µM of each primer and 5 µl of ten times PCR buffer (500 mM KCl and 200 mM Tris–HCl) and water to a total volume of 50 µl (Fig. 7).

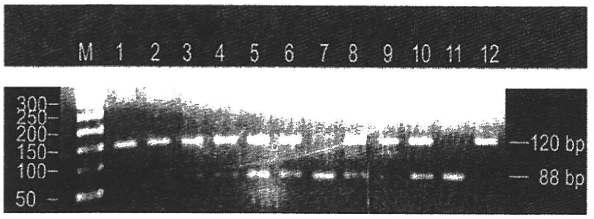

Fig. 8 RFLP-analysis of *CYP19* gene using SfaNI restriction enzyme. Lane M, 50-bp Marker (Invitrogen); lanes 1, 2, 9, 12, CC (120-bp); lanes 7 and 11, TT (88-bp); lanes 3–6, 8 and 10, CT (120, 88-bp)

Statistical analysis

In order to examine the association between the genotypes and the development of prostate cancer, we calculated odds ratio (OR) and 95% confidence interval (CI). The ORs were adjusted for age using multiple logistic regression analysis with computer software SPSS for Windows (version 11). Chi-square test was applied to compare the allelic frequencies between normal controls and prostate cancer patients. The $P < 0.05$ was considered statistically significant. The gene–gene interactions analysis was conformed using Epical 2004 (version 3.2.2).

Results

The allelic variants in the prostate cancer patients have been summarized in Table 2. The total incidence of the genotype containing −/− allele in *ERα* was higher in prostate cancer patients (18%) than in healthy individuals (10%). There was a threefold increased risk for prostate cancer in individuals carrying this genotype as compared to +/+ genotype (OR, 2.70; 95% CI, 1.08–6.70; $P = 0.032$). This was even evident when OR was adjusted for age (OR, 2.74; 95% CI, 1.10–6.84; $P = 0.030$). With regard to the +/− genotype, not much difference was revealed between groups of prostate cancer patients (54%) and control individuals (48%) and it was not statistically significant (OR, 1.68; 95% CI, 0.91–3.12; $P = 0.096$).

The prevalence of *Rr* genotype in *ERβ* was higher in prostate cancer patients (8.0%) as compared to controls (5.0%), but it was not statistically significant (OR, 1.65; 95% CI, 0.52–5.23; $P = 0.394$).

Among patients, the frequency of PR A1/A2 genotype was higher (16%) than controls (10%) and individuals carrying this genotype had a twofold higher risk for developing prostate cancer (OR, 1.71; 95% CI, 0.73–3.98; $P = 0.211$). The value was however not statistically significant. This was evident when OR was adjusted for age (OR, 1.74; 95% CI, 0.74–4.05; $P = 0.200$).

The frequency of *CYP19* CT genotype was higher in patients (37%) as compared to controls (20%) and this incidence was statistically significant (OR, 2.28; 95% CI, 1.20–4.35; $P = 0.012$). Stratification of patients according to age resulted in a slightly improved OR in individuals carrying CT compared to CC genotype (OR, 2.35 95% CI, 1.23–4.49; $P = 0.010$). There appeared to be an increased risk of prostate cancer associated with the Arg264Cys substitution in the *CYP19* gene.

Table 3 Distribution of combined allelic variants of *ERα* and *ERβ* gene in relation to *PR*, *CYP19* and *VDR* genotypes among prostate cancer patients and controls

Genotype		Cases	Controls	OR (95% CI)[a]	*P*-value
ERα	*ERβ*				
+/+	RR	24 (24%)	40 (40%)	1.00	
+/+	Rr	4 (4.0%)	2 (2.0%)	3.33 (0.56–19.59)	0.183
+/− + −/−	RR	68 (68%)	55 (55%)	2.06 (1.11–3.82)	0.022
ERα	PR				
+/+	A1/A1	26 (26%)	36 (36%)	1.00	
+/− + −/−	A1/A2	14 (14%)	4 (4.0%)	4.84 (1.43–16.42)	0.011
ERα	CYP19				
+/+	CC	16 (16%)	32 (32%)	1.00	
+/− + −/−	CC	43 (43%)	41 (41%)	2.09 (1.00–4.38)	0.049
+/− + −/−	CT + TT	29 (29%)	17 (17%)	3.41 (1.46–7.96)	0.005
ERβ	CYP19				
RR	CC	53 (53%)	15 (15%)	1.00	
RR	CT + TT	39 (39%)	26 (26%)	0.42 (0.19–0.90)	0.027
Rr	CC	6 (6.0%)	58 (58%)	0.02 (0.01–0.08)	0.001
ERβ	VDR				
RR	TT	52 (52%)	39 (39%)	1.00	
RR	Tt + tt	40 (40%)	56 (56%)	0.53 (0.30–0.95)	0.035

OR, odds ratio; CI, confidence interval

$P < 0.05$ was considered statistically significant

[a] ORs adjusted for age

The VDR tt genotype was not significantly associated with prostate cancer risk (OR, 0.43; 95% CI, 0.13–1.39; $P = 0.160$).

No association of *ERα/β*, *PR*, *CYP19* and *VDR* genotypes with prostate cancer risk was observed in relation to clinical stage (localized versus metastasis) and tumour grade (low grade <7 vs. high grade ≥7) (data not shown).

Combined genotype analysis

In the present case–control study by PCR-SSCP analysis, except some cases, no mutations either in DNA-binding (exons 2 and 3) or in hormone-binding (exons 4–8) domains were found, the association of the *ERβ*, *PR* and *CYP19* genotypes, which was evaluated with *ERα* genotype, is shown in Table 3. The heterozygous (+/−) and homozygous mutant (−/−) genotypes of *ERα* gene were combined as a single genotype and used for combination of this gene with other genes.

When the *ERα* was combined with *ERβ*, *PR*, *CYP19* and *VDR* genes, a few genotypes showed positive association and values are given in Table 3. Similarly, when *ERβ* was combined with *ERα*, *PR*, *CYP19* and *VDR* only three combined genotypes showed positive results (Table 4).

The frequency of *PR* gene for A1/A1 was 26% and 14% for A1/A2 alleles. A single copy of the variant allele, i.e. A1/A2 resulted in an OR of 4.84 (95% CI, 1.43–16.42; $P = 0.011$) as compared to the wild A1/A1 genotype when combined with mutant allele of *ERα* gene.

A threefold higher risk was observed when *ERα* and *CYP19* mutant genotypes were combined. It resulted in an OR of 3.41 (95% CI, 1.46–7.96; $P = 0.005$). The risk was also statistically significant when *CYP19* CC was combined with *ERα* mutant (OR, 2.09; 95% CI, 1.00–4.38; $P = 0.049$) genotype (Table 3). There was no association of the *VDR* genotypes with risk when combined with *ERα* gene.

The analysis of the combined *ERβ* genotypes in relation to different genes is given in Table 4. There was no risk of prostate cancer when *ERβ* was combined with *PR* and *CYP19* genes.

The role of *PR* gene in relation to *CYP19* genotype showed that there was no association of these two genes when combined together. There was a fourfold (OR, 3.72; 95% CI, 0.97−14.15) higher probability of prostate cancer risk in individuals having *PR A1/A2* and *VDR TT* in combined genotype.

A highly significant association was found in the combination of *CYP19* with *VDR* genotypes (Table 5).

Discussion

As many as 85 AR mutations are there in prostate cancer tissues [25], almost all being single-base substitutions due to somatic mutations, rather than germline mutations. These mutations are unequally distributed along the length of the AR and their types vary. In the present case–control

Table 4 Distribution of combined allelic variants of PR gene in relation to *CYP19* and VDR genotypes among prostate cancer patients and controls

Genotype		Cases	Controls	OR (95% CI)[a]	*P*-value
A1/A1	CC	50 (50%)	67 (67%)	1.00	
A1/A1	CT + TT	34 (34%)	23 (23%)	1.98 (1.04–3.77)	0.037
A1/A2	CC	9 (9.0%)	6 (6.0%)	2.01 (0.67–6.01)	0.212
A1/A2	CT + TT	7 (7.0%)	4 (4.0%)	2.34 (0.65–8.45)	0.193
A1/A1	TT	43 (43%)	40 (40%)	1.00	
A1/A1	Tt + tt	41 (41%)	50 (50%)	0.76 (0.42–1.38)	0.374
A1/A2	TT	12 (12%)	3 (3.0%)	3.72 (0.97–14.15)	0.054
A1/A2	Tt + tt	4 (4.0%)	7 (7.0%)	0.53 (0.14–1.95)	0.341

OR, odds ratio; CI, confidence interval

$P < 0.05$ was considered statistically significant

[a] ORs adjusted for age

Table 5 Distribution of combined allelic variants of *CYP19* gene in relation to *VDR* genotypes among prostate cancer patients and controls

Genotype		Cases	Controls	OR (95% CI)[a]	*P*-value
CC	TT	33 (33%)	64 (64%)	1.00	
CC	Tt + tt	26 (26%)	9 (9.0%)	5.60 (2.35–13.32)	0.00008
CT + TT	TT	23 (23%)	11 (11%)	4.05 (1.76–9.32)	0.001
CT + TT	Tt + tt	18 (18%)	16 (16%)	2.18 (0.98–4.82)	0.054

OR, odds ratio; CI, confidence interval

$P < 0.05$ was considered statistically significant

[a] ORs adjusted for age

study by PCR-SSCP analysis, except some cases, no mutations either in DNA-binding (exons 2 and 3) or in hormone-binding (exons 4–8) domains were found and it might be due to the small sample size. The mutations seen in exceptional cases on sequencing were found to be non-sense mutations.

The gene for the *ERα* has three known polymorphisms: PvuII, XbaI and B-variant polymorphisms, which are reportedly associated with receptor expression and altered receptor function and with some disorders including breast cancer, hypertension and spontaneous abortion. All three RFLPs are located in the A/B domain, the transactivating factor 1. It is an important site for stimulating transcription from certain estrogen-responsive promoters. Hernandez et al. [26] evaluated the association of the *XbaI* and *PvuII* ESR1 single nucleotide polymorphisms (SNPs) with the risk of prostate cancer in three different racial/ethnic populations of black, Hispanic white and non-Hispanic men. Allelic frequency was significantly different across ethnic/racial groups for both SNPs. No association was observed between Hispanic and non-Hispanic white men for this SNP. Also there was no association between the PvuII SNP and prostate cancer risk across all groups.

The analysis of *ERα* and detection of the PvuII restriction endonuclease showed that there was an increased risk associated with the −/− genotype with an OR of 2.70 (95% CI, 1.08–6.70; $P = 0.03$) and the result was statistically significant. The present results are in coherence with the observations of Suzuki et al. [27] who had found a significant association of the −/− genotyope of the PvuII site in the *ERα* gene in a study on 101 cases and 114 healthy individuals among Japanese population (OR, 3.44; 95% CI, 1.97–5.99; $P = 0.0028$). While in a case–control study by Modugno et al. [28], which was performed among Caucasian population of 88 prostate cancer patients and 241 male controls, no significant association was found between −/− and +/− genotypes of *ERα* gene. In a population-based case–control study in Sweden, Weiderpass et al. [29] had shown an association of PP (−/−) with a non-significantly decreased risk for endometrial cancer (OR, 0.70; 95% CI, 0.34–1.44) compared with the +/+ genotype. In another study of 1,069 breast cancer and 1,166 controls which was conducted in Urban Shanghai in China, there was an association of Pp (+/−) and pp (−/−) genotypes with an increased risk of breast cancer with age-adjusted ORs of 1.3 (95% CI, 1.0–1.7) and 1.4 (95% CI, 1.1–1.8), respectively, compared to *PP* (+/+) genotype [30]. Nonetheless, it has suggested a possible role for *ERα* in hormone-dependent tissues such as prostate and breast.

Although the frequency of *ERβ* Rr genotype was higher in prostate cancer patients as compared to controls, the *P*-value was not statistically significant. This observation showed that *ERβ* when analysed alone does not play an important role in the risk of prostate cancer in the present series of cases. Consistent with our results are the observations of Fukatsu et al. [31], who had found a non-significant association between *ERβ* gene and prostate cancer risk on 147 Japanese prostate cancer patients and 266 urological controls (OR, 0.73; 95% CI, 0.46–1.16; $P = 0.182$).

A polymorphism in intron G of the human progesterone caused by an Alu insertion was reported to be associated with ovarian carcinoma in a group of 67 patients of pooled German/Irish population [32]. Later on, a G to T substitution in exon 4, causing a valine to leucine change in the hinge region of the receptor, and a synonymous C to T substitution in exon 5, was linked to the Alu insertion [33]. The association of PROGINS with breast cancer was examined in North America (68 patients and 101 hospital controls) and in the south of England (292 patients and 220 healthy volunteers) [34, 35]. The allele frequency of PROGINS was slightly lower in the North American Caucasian breast cancer patients as compared with the hospital controls, but the difference was not statistically significant [36]. No difference between cases and controls was observed in the English study [34].

In the present study, no significant association with risk was found in the carriers of *PR* genotype and also on it combination with *CYP19* genotypes. An association was found with combined genotype of *PR* with *VDR* gene.

To date, several polymorphisms have been found in the *CYP19* gene. One of these, a C to T variation in exon 7 resulting in an Arg264Cys amino acid exchange, has been shown to be very common in Asia [37, 38] and could thus be an important modifier of breast cancer risk in the population in this area. The Arg264Cys polymorphism is located in or near recognition site of *CYP19* gene and thus it might enhance the estrogen synthesis and exposure to endogenous estrogen. However, it is also possible that *CYP19* Arg264Cys polymorphism is in linkage disequilibrium with other important polymorphic sites such as TTTA repeat polymorphism. In particular, alleles containing a high number of intronic TTTA repeats have been found to be over-represented in breast cancer patients as compared to controls [39, 40]. Monenen et al. [41] identified a novel SNP in the *CYP19A1* gene in prostate cancer. Individuals carrying the *CYP19A1* variant alleles had a significantly increased risk for prostate cancer (OR, 2.87; 95% CI, 1.10–7.49; $P = 0.03$). Lee et al. [39] had reported an association of *CYP19* Arg264Cys polymorphism with breast cancer in Korean women (OR, 1.5; 95% CI, 1.1–2.2) especially those consuming alcohol ($P = 0.04$). They demonstrated that *CYP19* might function as a low-penetrance gene in breast cancer genetic susceptibility.

In the present case–control study of north Indian population, an increased risk associated with *CYP19* CT

genotype was found and this association was statistically significant (OR, 2.28; 95% CI, 1.20–4.35; $P = 0.01$). Consistent with our results are the observations of Suzuki et al. [40] who had found an association of *CT* and *TT* genotypes of the *CYP19* gene (OR, 1.77; 95% CI, 1.02–3.09; $P = 0.037$) with prostate cancer risk among Japanese population. In another study, Modugno et al. [28] found that the *CYP19* CT genotype is associated with an increase in the risk of borderline significance (age-adjusted OR, 2.50; 95% CI, 0.99–6.28). These data suggested that *CYP19* gene could be used as an indicator for prostate carcinoma prevention in men in Asia.

In the present case–control study, there was an overall lack of association between the *VDR* TaqI polymorphism and the prostate cancer risk. In a hospital-based case–control study on a subgroup of whites, including 96 cases and 162 controls, Taylor et al. [22] had reported that men with the homozygous tt genotype were at decreased risk of developing prostate cancer compared with the TT or Tt genotypes (tt versus TT + Tt: OR, 0.32; 95% CI, 0.15–0.75; $P < 0.01$). In a larger case–control study among physicians' Health study on 372 incidents prostate cancer cases and 591 controls, Ma et al. [42] had observed no significant association of the investigated two *VDR* polymorphisms (TaqI and BsmI) and prostate cancer risk. Similarly, in a case control study consisting of 222 prostate cancer, 209 benign prostatic hyperplasia (BPH) and 128 male controls among Japanese populations, the TaqI polymorphism did not show any significant association with either prostate cancer or BPH [43]. Polymorphism in the *VDR* gene has been reported to be associated with prostate cancer in Indian population. The genotype frequency distribution between the prostate cancer and the control group was statistically significant ($P = 0.003$). Their study demonstrated that the FF genotype of the VDR gene plays an important role in determining the risk of prostate cancer and could be postulated as a good candidate genetic marker [44]. Blazer et al. [45] had also reported a lack of association between the TaqI genotype and the prostate cancer risk among 77 prostate cancer cases and 183 controls (tt versus TT + Tt: OR, 1.4; 95% CI, 0.7–2.8). A lack of association with VDR TaqI polymorphism was observed by Hamasaki et al. [46] among 115 cases and 133 age-matched controls. Similar observations were made by Figer et al. [47] among Israeli and Suzuki et al. [48] among Japanese patients. In a larger study of 1,870 prostate cancer cases and 2,843 controls on Greece population, comparison of tt and TT genotypes showed no difference in the frequency of these two genotypes in prostate cancer population (OR, 0.88; 95% CI, 0.70–1.10) [49]. The frequency of *VDR* genotype was not found to be significantly different between prostate cancer and male controls among Chinese population [50]. Huang et al. [51] had investigated the association of the BsmI, ApaI and TaqI polymorphisms of VDR gene with prostate cancer risk in a Taiwanese population. No significant association was found between the ApaI and the TaqI polymorphisms and the risk of prostate cancer. Similar observations had been made by other authors [52–55]. No statistically significant association of the *TaqI* polymorphism with prostate cancer was found in a study of 190 prostate cancer patients and 190 age-matched men with BPH (OR, 1.76; 95% CI, 0.90–3.45) [56]. There was no suggestion of an overall effect of TaqI polymorphism with prostate cancer susceptibility in subjects of European descent (OR, 0.97; 95% CI, 0.87–1.08), Asian descent (OR, 0.88; 95% CI, 0.66–1.17) or African descent (OR, 0.94; 95% CI, 0.41–2.17) [49]. In a case–control study of 368 prostate cancer patients and 243 BPH, no association was observed for TaqI polymorphism and risk of prostate cancer [54].

This is the first case–control study to our knowledge to examine the possible role of *ERs*, *PR*, *CYP19* and *VDR* genes in the development of prostate cancer in Indian men patients.

Taken together, these results clearly indicate that *ERα* and *CYP19* genes and to the lesser extent *ERβ*, *PR* and *VDR* genes in relation with other studied genes may be playing a role in prostate cancer risk. The small number of subjects in genotype subgroups may make the magnitude of our risk estimates uncertain; therefore, studies with a larger sample size are needed to clarify the complex interactions among the *ERα*, *ERβ*, *PR*, *CYP19* and *VDR* genes.

References

1. Chan MJ, Stampfer MJ, Giovannucci EL (1998) What causes prostate cancer? A brief summary of the epidemiology. Semin Cancer Biol 8:263–273
2. Bosland D (2000) The role of steroid hormones in prostate carcinogenesis. J Natl Cancer Inst Monogr 27:39–66
3. Mangelsdorf DJ, Thummel C, Beato M et al (1995) The nuclear receptor superfamily: the second decade. Cell 83:835–839
4. Fang S, Anderson KM, Liao S (1969) Receptor proteins for androgens. On the role of specific proteins in selective retention of 17-beta-hydroxy-5-alpha-androstan-3-one by rat ventral prostate in vivo and in vitro. J Biol Chem 244:6584–6595
5. Chang CS, Kokontis T, Liao ST (1988) Molecular cloning of human and rat complementary DNA encoding androgen receptors. Science 240:324–326
6. Lubahn DB, Joseph DR, Sullivan PM et al (1988) Cloning of human androgen receptor complementary DNA and localization to the X chromosome. Science 240: 327–330
7. Esteban E, Via M, Gonzalez-Perez E, Santamaria J et al (2005) An unexpected wide population variation of the G1733A polymorphism of the androgen receptor gene: data on the Mediterranean region. Am J Hum Biol 17(6):690–695
8. Green S, Walter P, Kumar V et al (1986) Human oestrogen receptor cDNA: sequence, expression and homology to v-erb-A. Nature 320:134–139

9. Mosselman S, Polman J, Dijkema R (1996) ER beta: identification and characterization of a novel human estrogen receptor. FEBS Lett 392:49–53
10. Ponglikitmongkol M, Green S, Chambon P (1988) Genomic organization of the human oestrogen receptor gene. EMBO J 7:3385–3388
11. Ogawa S, Hosoi T, Shiraki M et al (2000) Association of estrogen receptor β gene polymorphism with bone mineral density. Biochem Biophys Res Commun 269:537–541
12. Enmark E, Pelto-Huikko M, Grandien K et al (1997) Human estrogen receptor β-gene structure, chromosomal localization, and expression pattern, J Clin Endocrinol Metab 82:4258–4265
13. Rousseau MF, Misrahi M, Loosfelt H et al (1987) Localization of the human progesterone receptor gene to chromosome 11q22-q23. Hum Genet 77:280–282
14. Nebert DW, Nelson DR, Adesnik M et al (1989) The P450 gene superfamily: recommended nomenclature. DNA 8:1–13
15. Simpson ER, Mahendroo MS, Means GD et al (1994) Aromatase cytochrome P450, the enzyme responsible for estrogen biosynthesis. Endocr Rev 15:342–355
16. Voigt K, Bartsch W (1986) Intratissular androgens in benign prostatic hyperplasia and prostatic cancer. J Steroid Biochem 25:749–757
17. Gann PH, Hennekens CH, Ma J, Longeope C, Stampfer MJ (1996) A prospective study of sex hormone levels and risk of prosate cancer. J Natl Cancer Inst (Bethesda) 88:1118–1126
18. Hiramatsu M, Maehara I, Ozaki M et al (1997) Aromatase in Hyperplasia and carcinoma of the human prostate. Prostate 31:118–124
19. Ogawa S, Washburn TF, Taylor J et al (1998) Modifications of testosterone-dependent behaviors by estrogen receptor-α gene disruption in male mice. Endocrinology 139:5058–5069
20. Farnsworth WE (1996) Roles of estrogen and SHBE in prostate physiology. Prostate 28:17–23
21. Christakos S, Raval-Pandya M, Wernyj RP et al (1996) Genomic mechanisms involved in the pleiotropic actions of 1,25-dihydroxyvitamin D_3. Biochem J 316:361–371
22. Taylor JA, Hirvonen A, Watson M et al (1996) Association of prostate cancer with vitamin D receptor gene polymorphism. Cancer Res 56:4108–4110
23. Crofts LA, Hancock MS, Morrison NA et al (1998) Multiple promoters direct the tissue-specific expression of novel N-terminal variant human vitamin D receptor gene transcripts. Proc Natl Acad Sci USA 95:10529–10534
24. Bid HK, Mishra DK, Mittal RD (2005) Vitamin-D receptor (VDR) gene (Fok-I, Taq-I and Apa-I) polymorphisms in healthy individuals from north Indian population. Asian Pac J Cancer Prev 6(2):147–152
25. Gottlieb B, Beitel LK, Wu JH et al (2004) The androgen receptor gene mutations database (ARDB): update. Hum Mutat 23:527–533
26. Hernandez J, Balic I, Johnson-Pais TL et al (2006) Association between an estrogen receptor alpha gene polymorphism and the risk of prostate cancer in black men. J Urol 175(2):523–527
27. Suzuki K, Matsui H, Ohtake N et al (2003) Vitamin D receptor gene polymorphism in familial prostate cancer in a Japanese population. Int J Urol 10(5):261–266
28. Modugno F, Weissfeld JL, Trump DL et al (2001) Allelic variants of aromatase and the androgen and estrogen receptors: toward a multigenic model of prostate cancer risk. Clin Cancer Res 10:3092–3096
29. Weiderpass E, Persson I, Melhus H et al (2000) Estrogen receptor alpha gene polymorphisms and endometrial cancer risk. Carcinogenesis 21(4):623–627
30. Cai O, Shu XO, Jin F et al (2003) Genetic polymorphisms in the estrogen receptor alpha gene risk of breast cancer: results from the Shanghai breast cancer study. Cancer Epidemiol Biomarkers Prev 12:853–859
31. Fukatsu T, Hirokaw Y, Araki T et al (2004) Genetic polymorphisms of hormone-related genes and prostate cancer risk in the Japanese population. Anticancer Res 24:2431–2437
32. McKenna NJ, Kieback DG, Carney DN et al (1995). A germline TaqI restriction fragment length polymorphism in the progesterone receptor gene in ovarian carcinoma. Br J Cancer 71:451–455
33. Agoulnik I, Weigel N, Tong XW et al (1997) Functional analysis of mutated progesterone receptor that cosegregates with sporadic ovarian cancer. Proc Am Assoc Cancer Res 38:453
34. Manolitsas TP, Englefield P, Eccles DM et al (1997) No association of a 306-bp insertion polymorphism in the progesterone receptor gene with ovarian and breast cancer. Br J Cancer 75:1398–1399
35. Lancaster J M, Berchuck A, Carney ME et al (1998) Progesterone receptor gene polymorphism and risk for breast and ovarian cancer. Br J Cancer 78:277
36. Watanabe J, Harada N, Suemasu K et al (1997) Arginine-cystein polymorphism at codon 264 of the human *CYP19* gene does not affect aromatase activity. Pharmacogenetics 7:419–424
37. Kristensen VN, Andersen TI, Lindlom A et al (1998) A rare *CYP19* (Aromatase) variant may increase the risk of breast cancer. Pharmacogenetics 8:43–48
38. Haiman CA, Hankinson SE, Siegelmann D et al (2000) A tetranucleotide repeat polymorphism in *CYP19* and breast cancer risk. Int J Cancer 87:204–210
39. Lee MM, Gomez SL, Chang JS et al (2003) Soy and isoflavone consumption in relation to prostate cancer risk in China. Cancer Epidemiol Biomarkers Prev 12(7):665–668
40. Suzuki K, Nakazato H, Matsui H et al (2003) Genetic polymorphisms of estrogen receptor alpha, *CYP19*, catechol-O-methyltransferase are associated with familial prostate carcinoma risk in a Japanese population. Cancer 98(7):1411–1416
41. Mononen N, Seppala EH, Duggal P et al (2006) Profiling genetic variation along the androgen biosynthesis and metabolism pathways implicates several single nucleotide polymorphisms and their combinations as prostate cancer risk factors. Cancer Res 66(2):743–747
42. Ma J, Stampfer MJ, Gann PH et al (1998) Vitamin D receptor polymorphisms, circulating vitamin D metabolites, and risk of prostate cancer in United States physicians. Cancer Epidemiol Biomarkers Prev 7:385–390
43. Habuchi T, Liqing Z, Suzuki T et al (2000) Increased risk of prostate cancer and begin prostatic hyperplasia associated with a *CYP17* gene polymorphism with a gene dosage effect. Cancer Res 60:5710–5713
44. Mishra DK, Bid HK, Srivastava DS et al (2005) Association of vitamin D receptor gene polymorphism and risk of prostate cancer in India. Urol Int 74(4):315–318
45. Blazer DG, Umbach DM, Bostick RM et al (2000) Vitamin D receptor polymorphisms and prostate cancer. Mol Carcinog 27:18–21
46. Hamasaki T, Inatomi H, Katoh T et al (2002) Significance of vitamin D receptor gene polymorphism for risk and disease severity of prostate cancer and benign prostatic hyperplasia in Japanese. Urol Int 68(4):226–231
47. Figer A, Friedman T, Manguoglu AE et al (2003) Analysis of polymorphic patterns in candidate genes in Israeli patients with prostate cancer. Isr Med Assoc J 5(10):741–745
48. Suzuki K, Nakazato H, Matsui H. et al (2003) Genetic polymorphisms of estrogen receptor alpha, *CYP19*, catechol-O-methyltransferase are associated with familial prostate carcinoma risk in a Japanese population. Cancer 98(7):1411–1416
49. Ntais C, Polycarpou A, Ioannidis JP (2003) Vitamin D receptor gene polymorphisms and risk of prostate cancer: a meta-analysis. Cancer Epidemiol Biomarkers Prev 12(12):1395–1402